CHEMICAL REVIEWS

Volume 105, Number 8

Mechanochemistry: The Mechanical Activation of Covalent Bonds

Martin K. Beyer*,† and Hauke Clausen-Schaumann*,‡,§

Department Chemie, Technische Universität München, Lichtenbergstrasse 4, 85747 Garching, Germany, Institut für Strahlenschutz, GSF—Forschungszentrum für Umwelt und Gesundheit, GmbH, Ingolstädter Landstrasse 1, 85764 Neuherberg, Germany, and Munich University of Applied Sciences, FB 06, Lothstrasse 34, 80335 München, Germany

Received October 25, 2004

Contents

1. Introduction 2921
2. Macroscopic Phenomena 2922
2.1. Polymers under Mechanical Stress 2922
2.1.1. Homolytic Bond Cleavage of Polymers 2922
2.1.2. Mechanochemistry of Polymer Solids and Rubbers 2924
2.1.3. Bimolecular Reactions in Mechanochemistry 2925
2.1.4. Technological Relevance of Polymer Mechanochemistry 2926
2.2. Mechanochemistry of Crystals, Metals, and Alloys 2927
2.2.1. Brittle Fracture, Material Degradation, and Failure 2927
2.2.2. Mechanochemical Synthesis 2927
2.3. Mechanochemistry in Photochemistry 2928
2.3.1. Photochemical Degradation of Stressed Polymers 2928
2.3.2. Mechanochromism 2929
3. Single-Molecule or Single-Bond Studies 2930
3.1. From Ensemble Measurements to Single-Molecule Studies 2930
3.2. Single-Molecule Techniques in Force Spectroscopy 2930
3.3. Mechanical Rupture Forces of Single Chemical Bonds 2932
3.3.1. Covalent Bonds 2932
3.3.2. Metallic Bonds—Gold Nanowires 2937
3.3.3. Coordinative Bonds—Organometallic Bonds 2938
3.3.4. Charge-Transfer Complexes 2940
3.4. Knotted Polymers 2941
3.5. Theoretical Studies: Beyond Homolytic Bond Cleavage 2941
4. Conclusions and Outlook 2943
5. Acknowledgments 2944
6. References 2944

* To whom correspondence should be addressed. Telephone: ++49-89-289-13417. Fax: ++49-89-289-13416. E-mail: martin.beyer@ch.tum.de (M.K.B.); Telephone: ++49-89-1265-1417. Fax: ++49-89-1265-1480. E-mail: clausen-schaumann@fhm.edu (H.C.-S.).
† Technische Universität München.
‡ Institut für Strahlenschutz.
§ Current address: Munich University of Applied Sciences.

1. Introduction

Regarding the activation of chemical reactions, today's chemist is used to thinking in terms of thermochemistry, electrochemistry, and photochemistry, which is reflected in the organization and content of the standard physical chemistry textbooks. The fourth way of chemical activation, mechanochemistry, is usually less well-known. The purpose of the present review is to give a survey of the classical works in mechanochemistry and put the key mechanochemical phenomena into perspective with recent results from atomic force microscopy and quantum molecular dynamics simulations.

A detailed historical account on the development of mechanochemistry, with an emphasis on the mechanochemistry of solids, was recently given by Boldyrev and Tkáčová.[1] The first written document of a mechanochemical reaction is found in a book by Theophrastus of Ephesus (371−286 B.C.), a student of Aristotle, "De Lapidibus" or "On stones". If native cinnabar is rubbed in a brass mortar with a brass pestle in the presence of vinegar, metallic mercury is obtained. The mechanochemical reduction probably follows the reaction:[1−3]

$$HgS + Cu \rightarrow Hg + CuS \quad (1)$$

10.1021/cr030697h CCC: $53.50
Published on Web 07/19/2005

Martin Beyer received his diploma in physics in 1996 and a Ph.D. in physical chemistry in 1999 from TU Munich. With a Feodor Lynen fellowship from the Alexander von Humboldt foundation, he conducted postdoctoral research at UC Berkeley. In 2003, he received the Heinz Maier Leibnitz award jointly given by the Deutsche Forschungsgemeinschaft and the Bundesministerium für Bildung und Forschung. He finished his habilitation in 2004 and obtained the *venia legendi* in physical chemistry from TU Munich in the same year. Martin Beyer's research focuses on gas-phase ion chemistry of molecular and metal clusters, computational chemistry, and fundamental concepts in mechanochemistry.

Hauke Clausen-Schaumann studied physics at the Technical University of Munich. In 1995, he joined the group of Prof. Hermann Gaub, for his diploma research about the adsorption of DNA to nano-structured cationic lipid membranes. In 1996, he moved to the Ludwig Maximilians University in Munich, where he started his Ph.D. research in the area of single-molecule force spectroscopy. During this time, he also served as scientific coordinator of the national competence center for nanoanalytics. In 2000, he obtained his Ph.D. from the Ludwig Maximilians University, for his work on DNA mechanics. After several years as a scientist and R&D manager for private companies and public research organizations, he joined the Munich University for Applied Sciences as a Professor for nanobiotechnology, in October 2004. His research interests concern the mechanical properties of biomolecules and chemical bonds, the development of force-based biochip technologies, as well as biomembranes and single-enzyme activity.

Frequently, the introduction of the term mechanochemistry is attributed to Ostwald. While in his textbook on general chemistry, mechanical work is discussed in the context of the mechanical heat equivalent discovered by Mayer and Joule, we were unable to locate the alleged section on mechanochemistry in the volumes available to us.[4−6] Closest to mechanochemistry is his discussion of form energy and chemical energy in *Handbuch der allgemeinen Chemie*.[7] He envisions the displacement of unidentified internal parts of matter, causing the phenomena of internal friction and elastic deformation. He does not, however, explicitly discuss the possibility that mechanical force may directly induce chemical reactions. The origin of the term mechanochemistry thus remains obscure.

Today, mechanochemistry is an established field in material science and solid-state chemistry.[8] The Institute of Solid State Chemistry and Mechanochemistry in Novosibirsk, Russia, founded as the Chemical and Metallurgical Institute in 1944, carries its current name since 1997.[9] The International Mechanochemical Association (IMA) of the IUPAC initiated the International Conference on Mechanochemistry and Mechanical Alloying (INCOME),[10] which was held 4 times since 1993, with the last meeting thus far in Braunschweig, Germany, in 2003. From a different direction, the term mechanochemistry has recently been introduced in quantum molecular dynamics simulations of the pulling of gold nanowires in atomic force microscopy (AFM).[11]

The present review is restricted mostly to those mechanochemical phenomena, where identifiable strong, covalent chemical bonds are activated by the presence of an external mechanical force. Many solid-state phenomena are therefore excluded, like mechanically induced phase transitions under high pressure[12] and magnetization upon milling.[13] Unbinding and unfolding pathways of biomolecules, which could be loosely called "noncovalent mechanochemistry", have recently been reviewed[14−17] and are not in the focus of the current paper.

Fundamentals and applications of sonochemistry have recently been reviewed in depth by Thompson and Doraiswamy[18] and are therefore not included in the current review. The role of mechanochemistry in sonochemistry was recently discussed in detail by Luche.[19] According to Luche, true sonochemistry is the promotion of single electron transfers induced by ultrasonic waves, while mechanical effects of ultrasonic waves produce false sonochemistry. However, Boldyrev[20] as well as Nguyen et al.[21] present convincing evidence that mechanochemistry and sonochemistry are intimately related during cavitation collapse, because both phenomena occur under identical local conditions. The primary effect of sonochemistry in their view is cavitation, which provides the mechanical energy for all subsequent chemical reactions, including bond scission induced by viscous frictional forces.

Motor proteins,[22−27] the mechanochemistry of cytokinesis,[28] as well as synthetic and natural systems that generate mechanical strain as a response to a change in ion concentration[29] or temperature[30,31] are outside the scope of the present paper, as well as the modification of enzyme activity through a mechanic deformation of the macromolecule.[32,33]

2. Macroscopic Phenomena

2.1. Polymers under Mechanical Stress

2.1.1. Homolytic Bond Cleavage of Polymers

Staudinger[34−37] interpreted the reduction of the molecular weight of polymers under mastication as

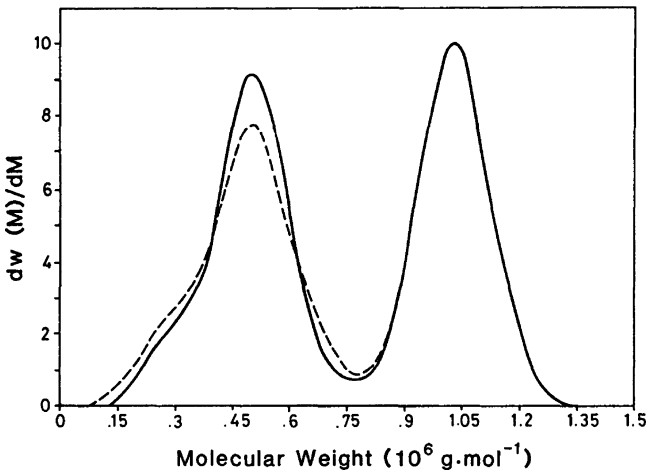

Figure 1. Molecular weight distribution of a polystyrene sample after degradation in decalin (—) and in 1-methylnaphthalene (- - -) under conditions of transient elongational flow. Fragments of 50 and 25% of the initial molecular weight are present, while there is a marked minimum at 75%. This clearly shows that polymers are ruptured in the center by viscous forces. Reprinted with permission from ref 40. Copyright 1990, American Chemical Society, Washington, DC.

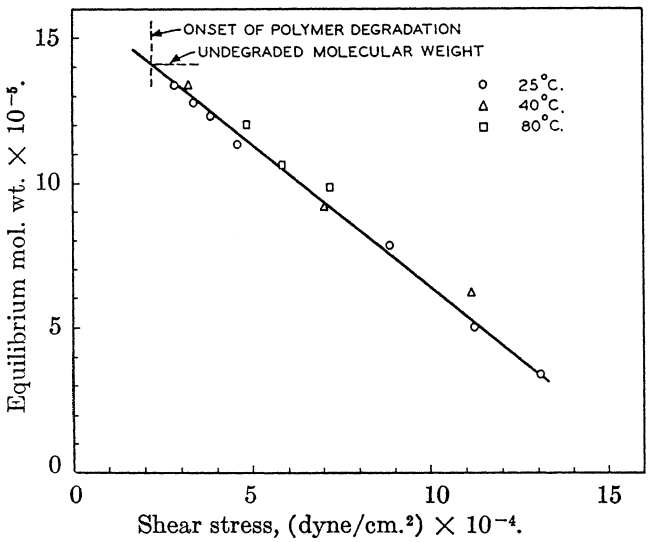

Figure 2. Degradation of 10% Vistanex 100 in cetane under laminar flow conditions. The data show a linear decrease of molecular weight with increasing shear stress, independent of the temperature. Reprinted with permission from ref 46. Copyright 1959, American Chemical Society, Washington, DC.

a mechanical rupture of the macromolecules. Kauzmann and Eyring[38] refined this idea, suggesting that shortening of polymers is caused by homolytic cleavage of the C−C bonds in the backbone under mechanical force, and described the rupture event with a Morse potential, which is gradually lowered by a linear potential, which originates from the external force. Frenkel in 1944[39] assumed that, above a critical velocity gradient, the polymer becomes partially uncoiled in the center and will rupture in this central position. In this model, each monomer unit experiences Stokes friction. In the center of the molecule, the force reaches its maximum, because all of the small contributions from the monomer units of the two halves work together. The central bond will experience the highest mechanical stress because of the viscous flow and has the highest probability to break. Experimentally, this midchain scission has frequently been verified, both as a flow-induced chain scission[40−42] and induced by ultrasonic cavitation.[43,44] Figure 1 shows recent results by Nguyen and Kausch on the molecular weight distribution of polystyrene under conditions of transient elongational flow.[40]

Because of the technological relevance of polymer stability, a significant number of studies on the degradation of polymers in solution by means of ultrasonic irradiation, shear forces in turbulent flow, and milling emerged, soon to be collected in a monograph by Jellinek.[45] Systematic studies of the degradation of polyisobutene in cetane by Porter and Johnson[46] established that similar effects are observed under laminar flow conditions. These authors concluded that the degradation process is rapid and terminates at an equilibrium polymer weight M, which decreases linearly with increasing shear stress, as illustrated in Figure 2.

This $1/M$ dependence of the critical strain rate for bond fracture was frequently observed in diverse polymer systems[47] and is clearly at odds with the $1/M^2$ dependence predicted by Frenkel for conditions of irrotational flow.[39] However, the calculation by Frenkel holds only for these specific flow conditions, which seem to be rarely met in experiments. Even for these exotic conditions, Frenkel made additional assumptions, because the purpose of his calculations was to rationalize the rupture events as such. Several steps in the derivation of the $1/M^2$ dependence are clearly marked as upper or lower limit estimates.[48] The obvious physically unreasonable consequences of his assumptions have been emphasized by Frenkel himself[39] and later by Rehner,[49] like the extension of the central polymer bonds to twice their original length. It seems that, after more than 60 years, there is still room for an exact theory of polymer midchain scission in viscous flow.

Harrington and Zimm undertook a kinetic study to elucidate the molecular mechanism of polymer degradation.[50] Their estimate of critical stresses on the individual bonds based on the experimental results was 2 orders of magnitude lower than the theoretical value of the maximum force in the inflection point of an analytic potential. They concluded that the main problem lies in the missing information about the actual mechanical stress in the rapidly flowing solutions. A major problem is that the assumption of laminar flow must be fulfilled and that turbulence will introduce a significant error. More recently, Odell et al.[51−54] constructed a cross-slot device to produce a planar elongational flow field. They corroborated the effect of chain halving. Data analysis with a modified Arrhenius rate equation allowed them to place the force required to rupture the chain in the range of 2.6−13.4 nN.[52]

In their experiments under conditions of transient elongational flow, Nguyen and Kausch find that the critical strain rate for chain rupture is only weakly dependent on the solvent viscosity.[40] They interpret these findings as bond activation by intramolecular friction between monomer units, which occurs only if the polymer is still coiled and the probability for

collisions between monomer units of the same molecule is high. At higher strain rates, also quasi-full-chain extension could be achieved in stagnant extensional flow.[55]

According to Nguyen and Kausch,[40,47] formation of free radicals by rupture of mechanically stressed chemical bonds was detected in many different states of aggregation, be it amorphous glasses, crystalline solids, rubbery states, melts, and solutions. Elongational flow fields such as the ones used by Odell et al.[51−54,56,57] provide idealized conditions for a quantitative investigation of the rupture of fully stretched polymers. Under less ideal conditions, like turbulent flow with high Reynolds numbers,[58,59] however, the residence time in the high strain rate zone is insufficient to fully stretch the molecule. This indicates that bond scission takes place in a predominantly coiled state.[40] The rate law follows a modified Arrhenius equation as proposed by Zhurkov,[60] in which part of the activation energy is supplied by mechanical work. Experimental observations that the rate of mechanochemical degradation is highest at low temperature[61,62] seemingly contradict this approach. This discrepancy is resolved if one considers the typically negative temperature dependence of viscosity in fluid systems: with increasing temperature, the higher mobility of the polymer and the solvent lead to less efficient coupling and a decrease in the frictional forces, which stretch the polymer.

Considerable effort has gone into an accurate theoretical modeling of polymer chains and chain fractures. The theory for flexible polymer chain dynamics in elongational flow is documented in a recent monograph by Nguyen and Kausch.[63] A historical account can be found in a 1994 publication by Doerr and Taylor.[64] The current level of sophistication is demonstrated in a series of papers from the last 15 years.[64−71] Typically, a one-dimensional chain of point masses is linked by equivalent bonds, which are described by an analytic potential. The analytic potential can be harmonic,[64−67] also termed Rouse chain,[65−67] a Morse potential,[65−67,70] or a Lennard−Jones potential.[68,69,71] Hydrodynamic interaction may be accounted for[66] as well as tunneling.[70] The applied force multiplied with the elongation is added to the binding potential, which generates a barrier. Transition-state theory is used to evaluate this problem.

2.1.2. Mechanochemistry of Polymer Solids and Rubbers

The mechanochemistry of polymer solids and rubbers, i.e., nonsolidified mixtures of macromolecules, exhibits a variety that goes far beyond the reactions documented in polymer solutions. This is probably due to the fact that the radicals formed remain localized and a larger number density of fractured bonds can be built up, as compared to elongational flow. A thorough understanding of mechanochemical reactions was reached a long time ago but goes virtually unnoticed in today's chemical literature, where the effect of using mortar and pestle in solid-state organic chemistry[72,73] is attributed to the generation of local heat.[73] This section is guided by three key papers,[60,74,75] which appeared in intervals of 15 years from 1959 to 1989.

Watson[74] starts his discussion with the mechanochemical degradation of rubber during mastication. In this process of cold-milling, the molecular weight of natural rubber is decreased by an order of magnitude from initial values of around 100 000 amu to achieve the desired viscoelastic properties. Mechanically induced homolytic cleavage of the C−C backbone bonds leads to formation of two free radicals[38,76] as the primary degradation step of elastomers. These radicals may recombine or disproportionate, react with oxygen from air, or attack other polymer molecules. With the help of radical acceptors, it was quantitatively shown that each rupture event produced radicals.[77] In the absence of radical acceptors, block or graft polymers may be formed. Watson's review ends with a bold statement,[74] envisioning that bimolecular reactions in mechanochemistry should be possible, which circumvent the formation of a pair of primary radicals. Because radical formation is a highly endothermic process, those mechanochemical reactions should be overall more readily activated than homolytic bond cleavage.

Zhurkov[78,79] developed a kinetic theory of the breakdown of solids, which is based on an experimentally established relationship between the lifetime of the material, the tensile stress acting on the material, and temperature. The modified Arrhenius equation mentioned already in section 2.1.1. accounts for the lowering of the activation energy by mechanical work

$$K = K_0 \exp[-(E_A - \alpha\sigma)/RT] \quad (2)$$

Tensile stress σ is measured in N m^{-2}, which gives the coefficient α the dimension of m^3 mol^{-1}, and their product is the mechanical work, which lowers the activation energy E_A. K_0 is the Arrhenius frequency factor, and K is the rate of bond-rupture events occurring in the polymer solid.

Electron spin resonance (ESR) studies by several groups[80−88] directly established the formation of radicals upon mechanically induced homolytic bond cleavage in macromolecules. These studies had also shown that free-radical generation increased exponentially with increasing tensile stress and temperature, in agreement with eq 2. Quantification, however, proved difficult because of the inherent instability of the primary radicals.

In their 1974 study of polyethylene and polypropylene solids,[60] Zhurkov and Korsukov quantified the formation of end groups upon bond rupture by infrared spectroscopy. In the polymer solid, the primary radicals undergo disproportionation to vinyl (R−CH=CH$_2$), vinylene (R$_2$C=CH$_2$), and methyl (R−CH$_3$) endgroups. In the presence of oxygen, also aldehyde (R−CHO) endgroups are formed. Each of these groups possesses a characteristic IR absorption band, which allowed quantification via difference spectra before and after exposing the sample to tensile stress for a defined time. The results showed that activation energies for macroscopic mechanical fracture, endgroup generation, and thermal degradation agree reasonably well, as shown in Table 1.[60]

Table 1. Activation Energies for Macroscopic Failure E_M, Microscopic Endgroup Formation E_E, and Thermally Activated Degradation E_T[a]

polymer	E_M	E_E	E_T
polyethylene (low pressure)	109	113	105
polyethylene (high pressure)	113	117	109
polypropylene	121	125	121

[a] All values in kJ mol^{-1}. Data taken from ref 60.

This study beautifully draws the line from macroscopic breakdown of a polymer solid to the failure of the individual interatomic bond and confirms the overall picture that homolytic bond cleavage is the starting point for the macroscopic process. The paper further discusses the role of microcrack formation in the breakdown of the macroscopic solid. Similar conclusions concerning the identification of endgroups were later also reached in an nuclear magnetic resonance (NMR) study by Kolbert et al.[89]

At the same time, the shift of vibrational frequencies in solids because of mechanical stress was observed.[90−95] Vettegren and Novak analyzed the change of conformational bands around 1000 cm^{-1} in polypropylene, poly(ethylene terephthalate), and nylon 6. They concluded that most of the bonds are uniformly stretched, while 6−30% experience a much higher load; i.e., they are "overstressed".[94]

Over the years, ESR became the primary, if not only, means of studying mechanochemistry of polymers. Sohma's 1989 review[75] describes carefully and concisely the methods used to produce mechanoradicals, like ball-milling, drilling, slicing, or sawing. While the ESR method immediately shows the formation of mechanoradicals, the direct proof of main-chain scission was more difficult. Figure 3 shows the ESR spectrum obtained from a polypropylene sample ball-milled at a temperature of 77 K in a vacuum, compared with a simulated spectrum obtained from a 1:1 mixture of the corresponding main-chain scission radicals.[96,97] This unambiguously shows that mechanical action generates equal amounts of the expected radicals, which is direct evidence for main-chain scission under mechanical stress. The review further discusses the formation of microcracks initiated by mechanoradicals and other phenomena, which lead to macroscopic degradation of polymer solids, as well as potential industrial applications of mechanochemistry. Mechanoradicals[98−105] and peroxy radicals as their secondary reaction products with oxygen[106] have continuously been observed by different groups in ESR experiments, leaving no doubt about the simple and intriguing fact that, whenever materials that consist of macromolecules, natural or artificial, are machined, sawed, or milled, radicals form by mechanical scission of covalent bonds.

2.1.3. Bimolecular Reactions in Mechanochemistry

In contrast to the large body of work on the breakdown of polymers, studies of bimolecular reactions under mechanical stress as envisioned by Watson[74] remained scarce. A review by Popov and Zaikov[107] lists only a handful of studies on the quantitative influence of mechanical stress on reaction kinetics, which, however, reveal key concepts

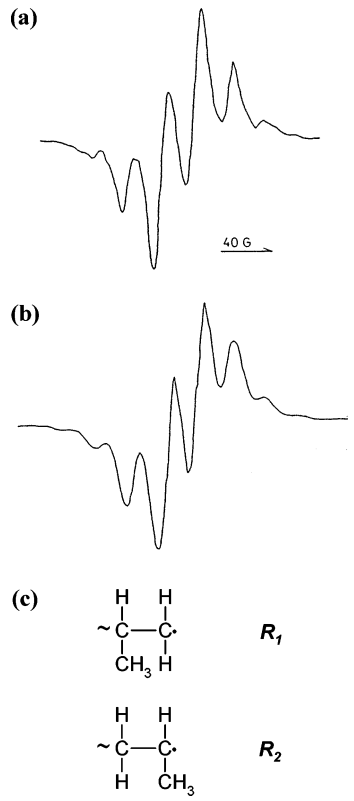

Figure 3. (a) Observed ESR spectrum of polypropylene, which was ball-milled at 77 K in vacuum. (b) Simulated spectrum obtained from a 1:1 mixture of the octet of radical R_1 and the quartet of radical R_2, shown in c. The excellent agreement is direct experimental proof of mechanically induced homolytic bond cleavage in polypropylene. Reprinted with permission from ref 75. Copyright 1989, Elsevier.

of mechanochemistry. Polyamide hydrolysis under ambient humidity was studied by Bershtein and Egorova.[108] They found that mechanical stress promoted the reaction and that the rate constant follows a rate law similar to eq 2. While ozonization of polyamide is insensitive to mechanical stress,[109] the same reaction is promoted for polypropylene.[110−116] Thermooxidation of polypropylene and polyethylene, on the other hand, is reduced by application of tensile stress.[117,118] The authors conclude[107,119] that the geometry changes during the reaction are responsible for this behavior, in what is essentially an application of le Chatelier's principle to mechanochemistry: If the reactive site is elongated during the reaction, tensile stress will increase and pressure will decrease the rate. If the reactive site is shortened in the course of the reaction, tensile stress will decrease and pressure will increase the rate.

Sohma reports the conversion of mechanoradicals in bimolecular reactions under mechanical stress.[75] Poly(methylmethacrylate) (PMMA) forms two mechanoradicals by main-chain scission, one of which is converted into a new radical by a bimolecular reaction with another polymer molecule, as shown in Scheme 1.[75,120] Sohma interprets this result in terms of the direct effect in mechanochemistry, which he considers as a process by which mechanical energy can cause chemical phenomena without any thermal path.

Scheme 1. Mechanochemical Formation of Primary and Secondary Radicals[a]

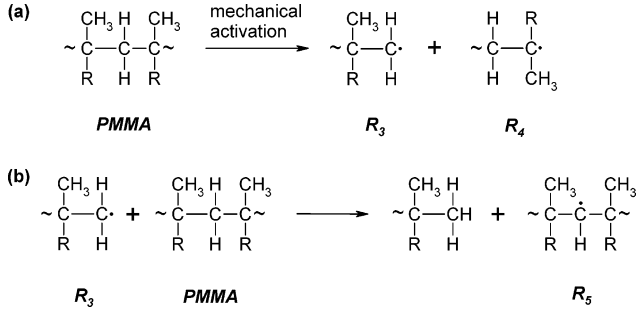

[a] (a) PMMA undergoes mechanically induced backbone scission, forming two distinguishable radicals R_3 and R_4; (b) radical R_3 abstracts a hydrogen atom from PMMA, resulting in a secondary radical R_5

The modified Arrhenius eq 2, however, implies that thermal activation is acting together with mechanical activation and that mechanical force is modifying the barriers of the bond-rupture process. This suggests that mechanical and thermal activation are not mutually exclusive. In general, mechanical force will lower the barrier for a particular reaction, be it unimolecular like chain rupture or bimolecular like the radical conversion. The final transition over the barrier, however, will in general be thermally activated. The crucial question is how does mechanical force modify the barrier?

2.1.4. Technological Relevance of Polymer Mechanochemistry

Mastication, which is the process where the concept of mechanochemistry was first developed, still is the method of choice for the treatment of natural rubber to reach desired rheological properties.[76,121−127] Its direct effect is shortening of the polymer chains by homolytic bond cleavage, which affects the viscosity of the material. Mechanical and thermo-oxidative breakdowns are the two accepted mechanisms involved.[121] The mechanical effect of extruder action is in general quantified in terms of specific energy and not force, which would seem the more appropriate measure. Interestingly, it is known that mastication agents such as oxygen or pentachlorthiophenol derivates accelerate molecular degradation during the mastication process.[122] The accepted mechanism for this process is that the mechanoradicals generated by homolytic bond scission activate the mastication agents. However, why this should lead to accelerated degradation is not obvious. It seems promising to investigate if mechanically activated but not yet ruptured bonds are directly attacked by the mastication agents, as outlined in section 2.1.3. for other systems.

Mechanochemical treatment is possible for synthetic polymers such as polystyrene and PMMA and leads to reduced molecular nonuniformity in comparison with the educt. Polydispersities less than 1.3 can be achieved.[128,129]

Besides the seemingly purely destructive process of mastication, recent efforts demonstrate the feasibility of using mechanoradicals for controlled polymerization and copolymerization by grinding and milling.[130−141] Schmidt-Naake and co-workers demonstrated the controlled synthesis of block and graft copolymers in a vibratory mill.[132,135] Graft-modified highly chlorinated polyethylene with methylmethacrylate was prepared mechanochemically by Zhao et al. and showed promising material properties.[142] Crosslinking was observed upon mechanical milling of polyisoprene at cryogenic conditions by Spontak and co-workers.[130] In the recycling of polymeric waste by shear pulverization, formation of mechanoradicals is probably a desired effect, which aids the *in situ* compatibilization of commingled plastic waste by formation of block and graft copolymers.[143,144] Mechanochemical solid-state polymerization was also used in prodrug syntheses by Kuzuya and coworkers.[145−150]

Mechanochemistry is also employed in the development of biodegradable resins. Biodegradable soy protein−polyester blends have been prepared in a reactive extrusion process, using glycerol as a compatibilizing agent.[151] It was found that high shear mixing led to thermoplastic blends characterized by high elongation and high tensile strength.

Mechanochemical treatment of hazardous polyhalogenated contaminants, like PCBs, PCP[152] or DDT,[153] results in significant dehalogenation of the hazardous substance. Contaminated materials as well as highly concentrated or pure contaminants are treated at room temperature by ball milling in the presence of magnesium, aluminum, or sodium and an acidic hydrogen source.[152] The process is designed to be part of recycling schemes, in which toxic compounds may be converted into defined and usable products.

Lubricants are used to optimize energy efficiency and minimize wear in the machinery, which they lubricate.[154] Perfluoropolyether lubricants are used in magnetic storage devices and are subject to degradation under sliding conditions.[155] Polymer-bearing surfaces are similarly subject to shear and frictional forces.[156] Friction processes and mechanisms are studied experimentally with the surface force apparatus[157,158] and computationally with molecular dynamics simulations.[159] Friction is responsible for the build-up of shear forces, which lead to wear of the machinery but also of the lubricants themselves, analogous to the mastication process. Mechanochemical concepts might be valuable to describe and understand these exceedingly complicated and subtle processes.[160] Recently, the application of density functional theory based concepts in lubrication chemistry was reviewed by Shenghua et al.[161]

Degradation of polymer solids by mechanical stress is an obvious technical aspect of mechanochemistry and has been studied in great detail.[162] It was observed that scissions of chemical bonds accumulate in the surface layer, which is attributed to the heterogeneity of external load distribution over chemical bonds near the surface.[163] Indirectly, mechanical deformation and resulting stress is operational in the low-temperature degradation of polymers in solution. When polystyrene solutions were subjected to 45 freezing cycles, the molecular weight was reduced

from the initial value of 7.3×10^6 amu by a factor of 3.[164]

Long-term mechanical degradation of polymers is potentially relevant in medicine. Resistance to wear is an important factor in determining the clinical success of dental resin composites,[165] where the phenomenon of fatigue likely includes mechanochemical degradation. Biopolymers present in the synovial fluid for joint lubrication[166,167] should be especially stable against mechanically induced degradation.

Mechanochemical treatment of biopolymers has been studied for the last 20 years in food technology.[168−176] Macromolecular degradation of starch to obtain a desired molecular weight is of interest for product-oriented process design and for new products in food industry. Boom and co-workers have in a series of studies presented evidence that mechanochemical degradation is operative in the typical extrusion process.[174−176] Also proteins are subjected to extrusion, e.g., whey protein, which is a byproduct of the cheesemaking process.[173] Free-radical formation, a distinct feature of shear-induced bond scission, was recently observed by ESR spectroscopy in the extrusion of wheat flour protein.[172]

2.2. Mechanochemistry of Crystals, Metals, and Alloys

The prospects and problems of future developments in mechanochemistry have recently been discussed by Butyagin,[177,178] Boldyrev and Tkáčová,[1,179] and Baláž.[2] In solid-state mechanochemistry, nonthermal chemical reactions occur because of the deformation and fracture of solids, which are technically induced by milling or grinding of the material. Figure 4 shows various types of mills used for these purposes. In this sense, mechanochemical activation precedes the reaction and involves the increase of internal and surface energy, increase of surface area, and decrease of the coherence energy of solids.[2] In a second step, these may lead to spontaneous aggregation, adsorption, or recrystallization in the activated system, which may appear during grinding or after grinding has been completed.

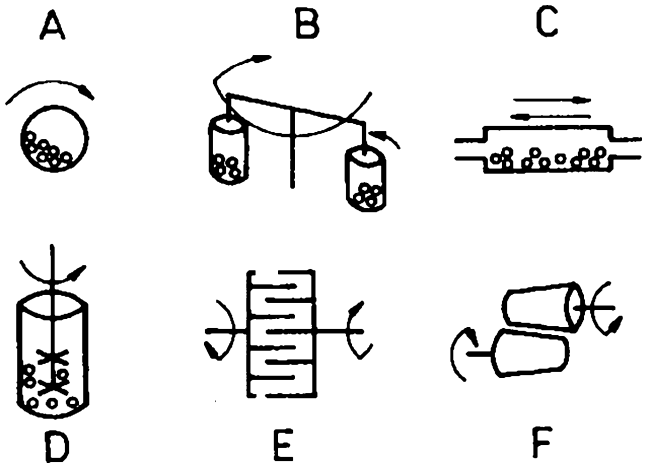

Figure 4. Types of mills for mechanical activation. (A) Ball mill. (B) Planetary mill. (C) Vibratory mill. (D) Stirring ball mill (attritor). (E) Pin mill. (F) Rolling mill. Reprinted with permission from ref 2. Copyright 2003, Elsevier.

2.2.1. Brittle Fracture, Material Degradation, and Failure

Fracture of solids by milling or grinding is used to activate surfaces for various applications. Zeolithes have been milled together with phosphates to generate aluminum-containing active centers, which interact with phosphate anions.[12] This effect may contribute to phosphate fixation and increase the efficiency of fertilizers while reducing the contamination of groundwater.

However, also undesirable effects of mechanical surface activation are discussed. Mineral dust generated during sandblasting or milling may carry free radicals on the surface, which react with ambient substances to generate highly reactive centers.[180] When inhaled, this effect may determine drastically the pulmonary toxicity of the particulate mineral.

Another "green" aspect of mechanochemistry is the preparation of catalysts by mechanochemical methods. Molchanov and Buyanov review waste-free energy-saving methods for the preparation of hydride catalysts, heteropoly acid catalysts, and catalysts for hydrocarbon decomposition. Mechanochemical methods may modify the properties of catalysts as well as supports and lead to improved catalytic activity and sorption properties.[181] To elucidate this effect, Mitchenko et al. studied mechanically induced reactions of platinum complexes.[182] They found that mechanical treatment of solid K_2PtX_6 (X = Cl, Br) leads to homolytic cleavage of Pt−X bonds and formation of K_2PtX_5 along with X_2 molecules.

2.2.2. Mechanochemical Synthesis

Mechanochemical processing is a powder metallurgy process, in which the application of mechanical energy induces chemical reactions and phase transformations. Mechanical alloying is a powder-processing technique involving deformation, cold welding, fracturing, and rewelding of powder particles in a ball mill. Both processes have recently been reviewed in detail by Ivanov and Suryanarayana.[183] Apart from the basic ideas, these authors also present actual industrial application of the two processes, such as oxide-dispersion strengthened (ODS) alloys and physical vapor deposition (PVD) targets.

A substance class whose mechanochemistry is particularly well-understood are spinel ferrites, $MeFe_2O_4$, where *Me* represents a divalent transition metal cation, as studied by Šepelák, Becker, Steinicke, and co-workers.[184−191] High-energy milling in a stainless-steel vial reduces the average crystallite size of $MgFe_2O_4$ to the nanometer range.[185] Prolonged mechanical milling leads to chemical reduction and formation of a solid solution of FeO and MgO, with metallic iron as a byproduct, as evidenced both by Mössbauer spectroscopy and X-ray powder diffraction.[185]

Mechanochemistry is also frequently investigated in the area of hydrogen chemistry and hydrogen storage in metal-containing solids.[192] Ball milling for the synthesis of doped sodium alanate was introduced in 1999[193,194] and is now widely used.[195,196] However, ball milling in turn may lead to catalytic decomposition of $NaAlH_4$.[197] Recently, also,

$Mg(AlH_4)_2$,[198] $Ca(AlH_4)_2$,[199] and $Sr(AlH_4)_2$,[200] as well as lithium beryllium hydrides $Li_nBe_mH_{n+2m}$,[201] have been prepared mechanochemically. Zr-based alloys change their hydrogen adsorption characteristics upon milling.[202] Only prolonged milling leads to H_2 elimination from $LiAlH_4$, as reported by Balema et al.[203] They attribute this to the catalytic effect of iron, which is introduced as a contaminant during the mechanical treatment. H_2 release upon dry grinding of kaolinite was reported by Kameda et al.[204] H_2 forms through the reaction between surface water molecules and mechanoradicals created by the rupture of Si−O or Al−O−Si bonds. The H_2 concentration increases as long as the grinding continues, which suggests that mechanoradicals are also continuously formed. In turn, it was suggested by Kameda et al. that H_2 formation may be used as an indicator for the formation of mechanoradicals.

Even more intriguing is the formation of methane and ethane in the mechanical treatment of $NiZrH_x$, ZrH_x, NiZr, Zr, Ni, or Zr + Ni in the presence of CO + H_2, CO, or graphite.[205,206] In the mixture of hydrides with carbon, 100% of the hydride may be converted into methane. The opposite behavior is observed upon ball milling of the aromatic hydrocarbons biphenyl, naphthalene, anthracene, and phenanthrene, which are converted to graphite.[207]

Mechanochemistry is also potentially important in atmospheric chemistry, i.e., for the concentration of trace gases in the atmosphere. Martinelli et al. report that, upon grinding in a ring-roller mill, calcium carbonate in the form of calcite loses crystallinity and an abundant release of CO_2 is observed. The authors suggest that this mechanochemical route could play an important role in the natural release of CO_2 into the earth's atmosphere.[208] Nikolaev et al. discuss the possible role of mechanochemistry in the methane balance of the earth's atmosphere.[209]

Reactions within or between molecular crystals, which are activated by mechanical methods, have recently been reviewed by Braga and Grepioni.[210] They conclude that solvent-free mechanical methods, such as cogrinding, milling, and kneading, represent promising routes for the preparation of novel molecular and supramolecular solids. Hybrid organic−organometallic materials are obtained by manual grinding of an organometallic complex with a number of solid bases in a solvent-free reaction, which involves molecular diffusion through the lattice, breaking and reassembling of hydrogen-bonded networks, as well as proton transfer.[211] Kolotikov et al. report the mechanochemical synthesis of tris(pyrazolylborate) complexes of Mn^{II}, Co^{II}, and Ni^{II}.[212] Interestingly, they also observe the formation of a substituted pyrazole ligand, which results from hydrolysis of the corresponding tris(pyrazolylborate). Hydrolysis seems to be a frequent reaction in mechanochemistry.

Mechanochemical synthesis of fullerene compounds has recently been reported by Braun,[213,214] Komatsu and co-workers,[215−231] and Constabel and Geckeler.[232] Single-walled carbon nanotubes and cyclodextrins mixed by high-speed vibration milling are water-soluble, which was attributed to the formation of nanotube−cyclodextrin complexes and the debundling of the nanotubes.[219] Strained single-walled carbon nanotubes experience oxidative acid attack, as observed by Ausman et al.,[233] leading to the etching of the kinked sites of the nanotube. This may be an example of the theoretically proposed effect that mechanical strain increases the proton affinity of binding sites.[234] The strength and breaking mechanisms under high tensile load of films[235] and ropes[236] of single-wall carbon nanotubes, as well as multiwalled carbon nanotubes,[237] have recently been investigated.

Coal can be activated by milling or grinding, as reported by Heegn[12] and Turcaniova and Baláž.[238] Heegn suggests that mechanical rupture causes the formation of radicals, which react with oxygen or water to basic or acidic groups. The process promises to yield activated coal powders at a competitive price and higher quality than thermal activation procedures.[12]

Olefines can be mechanochemically oxidized to carbonic acids with potassium permanganate in a solvent-free environment, as found by Nüchter et al.[239] The presence of water was found to enhance the product yield. Again, the influence of water indicates that hydrolysis plays a role in this process. Grinding of crystalline organic acids and amines leads to proton transfer with ammonium salt formation or to hydrogen-bonded complexes.[240]

Mechanochemical reactions may also be induced by milling and pressing of analytes with KBr to form a disk for IR spectroscopy, resulting in a change of the spectrum of the analyte. This effect has been known for long, and the literature was recently reviewed by Fernandez-Bertran.[241] Research in this area is ongoing.[242]

2.3. Mechanochemistry in Photochemistry

2.3.1. Photochemical Degradation of Stressed Polymers

Sohma observed an enhancement of the photodegradation of polypropylene after passing through an extruder.[243] He attributed this to the formation of ketones in the fractured samples, which act as chromophores. This result is important for the material properties of mechanically treated polymers in general, especially with regard to mechanical treatment in polymer recycling.

The photolysis of polymer materials is more complex and multifaceted while they experience mechanical stress.[244−260] It is well-known that tensile stress accelerates the photodegradation of polyolefins,[245−252,254,258] polycarbonates,[246] nylon,[253,256] and acrylic-melamine coatings,[257] while photodegradation is in general slowed by compressive stress.[247] The technical importance of these phenomena is obvious, because many polymers are exposed to light and at the same time mechanical stress. Recently, Tyler and co-workers[244] discussed the available theories for the synergism between light and stress. The Plotnikov hypothesis[261] assumes that stress lowers the activation barrier for bond dissociation in the excited state and thus increases the quantum yield Φ (Figure 5a).

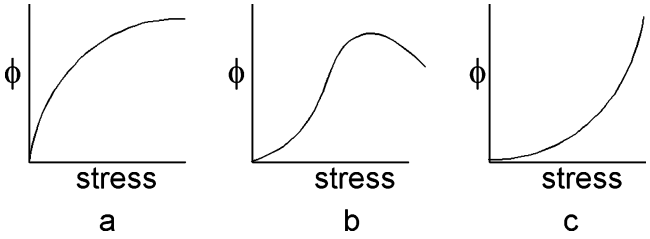

Figure 5. Expected quantum yield for degradation versus mechanical stress according to three different models: (a) the Plotnikov equation, (b) the DREE hypothesis, and (c) the Zhurkov equation. Reprinted with permission from ref 244. Copyright 2004, American Chemical Society, Washington, DC.

The "Decreased Radical Recombination Efficiency (DRRE) Hypothesis", put forward by several authors,[248,262,263] assumes that the effect of stress is divided into four stages, which represent morphological transitions in the sample. Initially, photodegradation quantum yield increases with stress, which is attributed to the decreased recombination efficiency of the radicals generated by photolysis, because they are separated by the applied stress. The decrease predicted in a later stage in this hypothesis is due to a higher degree of orientation in the system, which reduces diffusion of radical traps such as oxygen and in turn increases the probability of radical recombination (Figure 5b). Finally, also a modification of the Zhurkov eq 2 was put forward, using an effective activation energy (Figure 5c).

Chen and Tyler studied the photochemical degradation of two stressed poly(vinyl chloride)-based polymers, which contain Mo−Mo bonds along the backbone.[244] The device used is shown in Figure 6.

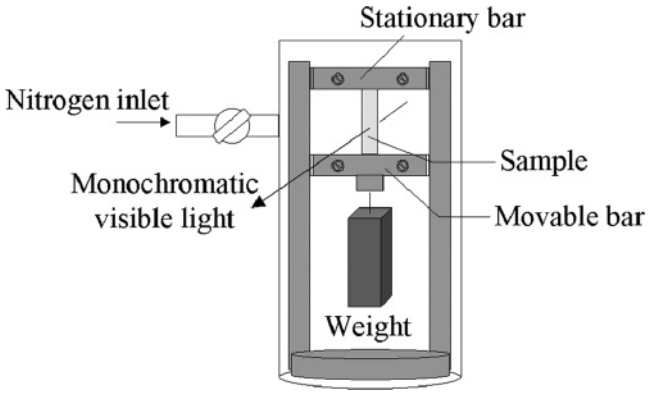

Figure 6. Device used to stress polymer films anaerobically during irradiation. The apparatus is enclosed in a glass container that is filled with nitrogen. Reprinted with permission from ref 244. Copyright 2004, American Chemical Society, Washington, DC.

Anaerobic stretching of a polymer film sample during irradiation is achieved in a nitrogen atmosphere, and the construction allows for simultaneous irradiation and analysis by FT-IR spectroscopy. Figure 7 shows the quantum yield for the degradation of one of the studied polymers as a function of tensile stress, and the other polymer yielded a similar pattern. The photodegradation quantum yield quickly reaches a maximum, followed by a marked decrease, which is in accordance with the DRRE hypothesis. However, none of the other hypotheses are conclusively ruled

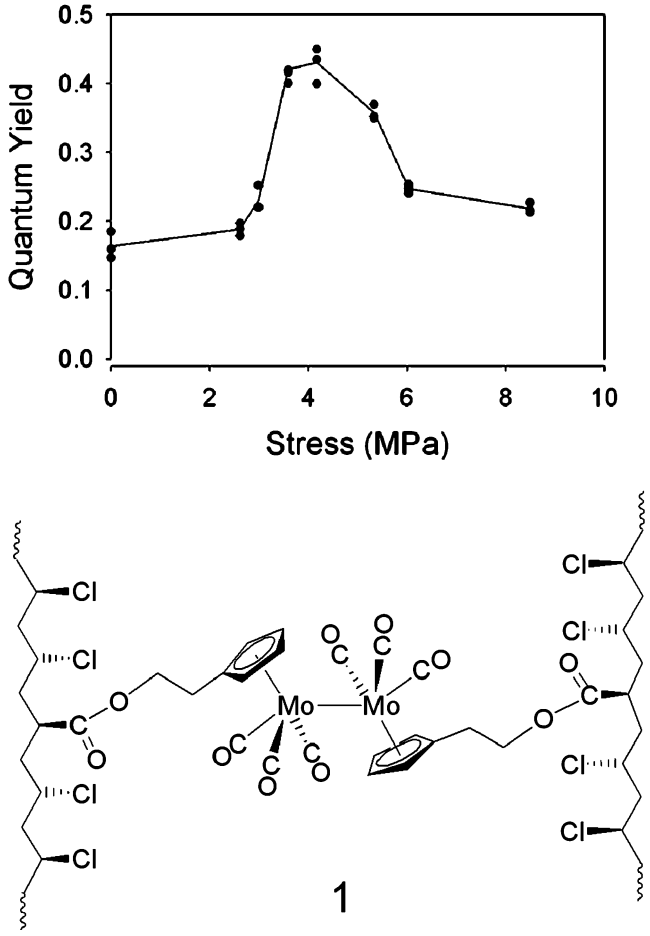

Figure 7. Quantum yields for degradation of **1** versus applied tensile stress. The results of three independent measurements at each stress are shown. Reprinted with permission from ref 244. Copyright 2004, American Chemical Society, Washington, DC.

out, because other effects are still possible in this exceedingly complex situation of a mechanically stressed polymer solid under irradiation with light.

2.3.2. Mechanochromism

Mechanochromic transitions of organic compounds have recently been reviewed by Todres.[264] The term mechanochromism is used for mechanically induced color changes. Examples are spectral changes as a result of mechanically induced reorganization of crystal packing or mechanically induced structural phase transitions, as well as triboluminscence, which is the emission of light by solids when they are stressed or fractured. A particularly illustrative example of mechanochromism, which is potentially useful for teaching in, e.g., organic chemistry lab class, is the change of color upon mechanically induced bond breaking or isomerization.

In the simplest case, mechanically induced homolytic bond cleavage leads to the formation of two colored radicals, e.g., when the unpaired electron is placed in a suitable aromatic system.[264,265] A different example of mechanochromism is found in spiropyrans, where ring opening by breaking the weak bond between the nodal carbon atom and the ethereal oxygen is accompanied by a change of color from

Scheme 2. Mechanochromism in Spiropyran[a]

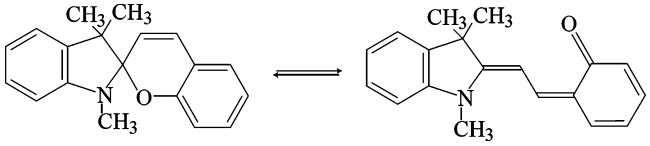

[a] Ring opening by breaking the weak bond between the nodal carbon atom and the ethereal oxygen is accompanied by a change of color from yellow to blue. Reprinted with permission from ref 264. Copyright 2004, Science Reviews.

yellow to blue.[264,266] This ring opening, shown in Scheme 2, can be induced thermally or by photon absorption, selective solvation, or grinding. The mechanochromic effect observed upon grinding is enhanced at low temperatures, which indicates that ring opening is genuinely activated by a mechanical force and not indirectly by frictional heat.

The reverse effect, the driving of mechanical actuators with light, was also demonstrated experimentally, on the single-molecule level by Hugel et al.[267] and macroscopically by Athanassiou et al.[268] The color change of organic chromophores under tensile stress was recently investigated with semiempirical methods by Frank and co-workers.[269]

3. Single-Molecule or Single-Bond Studies

3.1. From Ensemble Measurements to Single-Molecule Studies

Although force is an important functional and structural parameter,[270] characterizing chemical bonds, traditionally, the "binding force", has been determined only indirectly, i.e., by measuring resonance frequencies ω of molecular bonds with optical spectroscopy. The force constant k of the bond corresponds to the curvature of the potential in its minimum. In the harmonic approximation, ω and k are linked via the reduced mass μ of the oscillator

$$\omega = \sqrt{k/\mu} \tag{3}$$

Because of the scalar nature of the observable frequency, no synchronization of molecules is required to determine it from ensemble measurements. Force, however, has a direction, and in an ensemble with an isotropic distribution of force vectors, the average force always vanishes. Therefore, synchronization in space and time is necessary for a direct quantification of binding forces in ensemble measurements. This synchronization requires considerable experimental effort, and usually only a certain fraction of the bonds probed is actually aligned and synchronized in the appropriate fashion. At the same time, the mechanical failure of bulk material is a rather complex process, and the number of bonds rupturing at a given time, their angular distribution, and the role of shear forces and friction are difficult to asses. Therefore, it remains challenging to relate rupture forces determined in bulk material to the rupture forces of individual chemical bonds.

The introduction of the surface force apparatus (SFA) in the early 1970s by Tabor and Israelachvili[158,271] somewhat simplified the quantification of bond-rupture forces. At an interface, the separation process can be much better controlled than in bulk material, and the number of bonds failing at a given time can be greatly reduced. In the SFA, only bonds at the rim of the contact area contribute to the measured force. Nevertheless, the exact quantification of bonds contributing and the separation of short-range chemical forces and long-range forces, such as van der Waals forces and electrostatic forces, remain difficult. The SFA has been used extensively to assess hydration and colloidal forces,[272] as well as friction[273] and biochemical bonds.[274] However, to our knowledge, no measurements of covalent binding forces have been reported with the SFA.

New single-molecule techniques, which have been developed over the past 15 years, allow for the measuring of the mechanical properties of individual molecules and bonds directly. Therefore, a synchronization of molecules is no longer necessary, and the interpretation of the data is straightforward. Owing to the simplicity of this approach, within the past decade, this field has grown rapidly and a vast number of natural and synthetic molecules and bonds have been studied using single-molecule force spectroscopy. In the beginning, home-built instruments were used in these studies. Recently, suitable commercial instruments have become available, and now more and more investigators from chemical and life sciences are joining this field. From polymer elasticity[275−277] to molecular motors,[278,279] from DNA base pairing[280−284] to protein folding,[15,16,285,286] and from molecular recognition[287,288] to chemical binding, single-molecule studies, together with theoretical modeling, have provided new insights into the mechanisms governing these phenomena at the molecular level.

The vast majority of these studies, as well as the majority of review articles, deals with biomolecules or with the elastic response of polymeric material. However, today there is an increasing number of experimental and theoretical work devoted to the investigation of covalent, metallic, and coordinative chemical binding. In the current section 3, we summarize these findings and put them into perspective with the traditional methods in mechanochemistry discussed in section 2. For other aspects of single-molecule force spectroscopy, we refer the reader to the numerous review papers available in the field.[14,17,289−309] A very comprehensive account of force spectroscopy with biomolecular bonds is the review by Merkel.[17] Life science and material science aspects are covered in the paper by Hugel and Seitz[295] and a book chapter by Seitz.[310] An excellent introduction to the relation between strength, lifetime, and structural parameters of single-molecular bonds can be found in the review by Evans.[293]

3.2. Single-Molecule Techniques in Force Spectroscopy

The techniques used in single-molecule mechanics include optical and magnetic tweezers, glass microneedles, the biomembrane force probe (BFP), hydrodynamic methods, and techniques based on the atomic force microscope (AFM). Figure 8 illustrates the force range of interest in single-molecule force

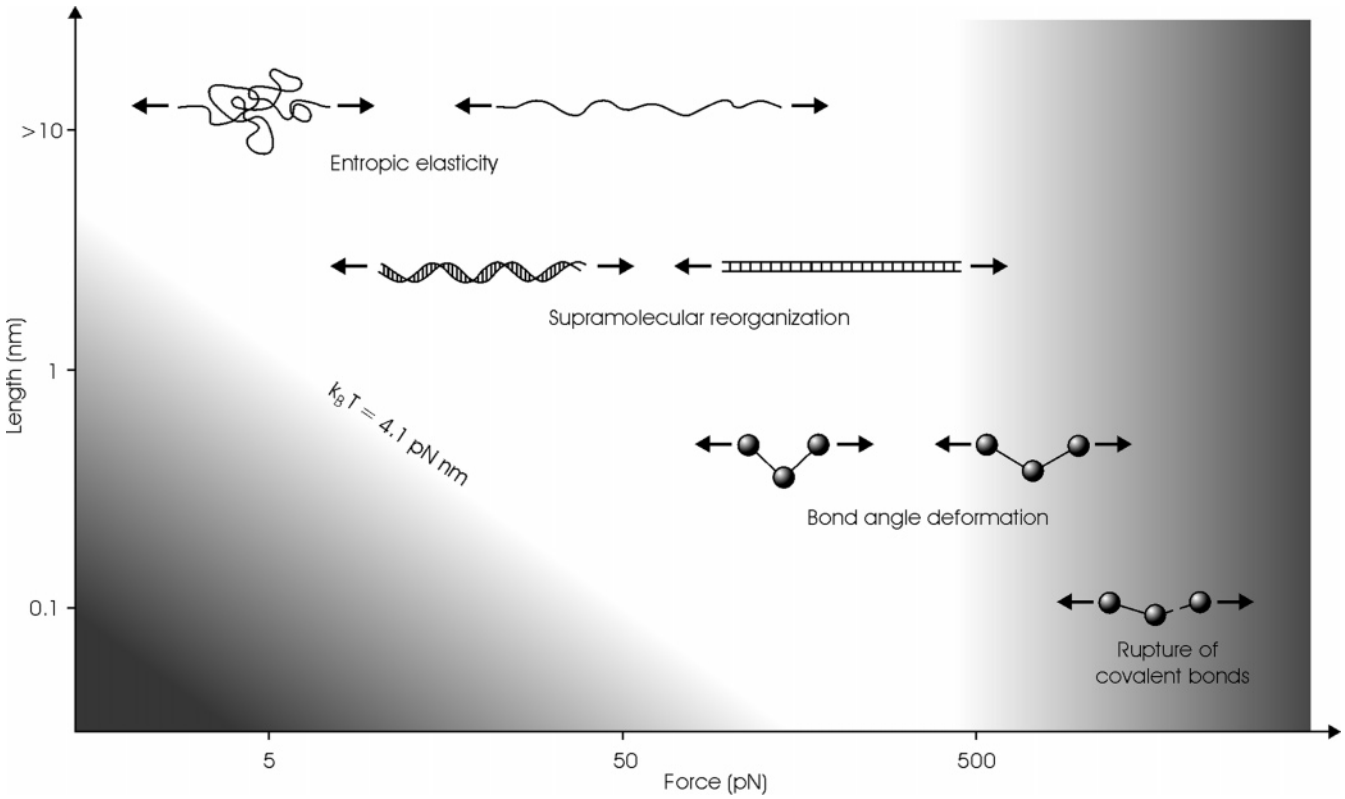

Figure 8. Accessible force range in single-molecule force spectroscopy. The thermal energy k_BT, which equals 4.1 pN nm at room temperature, defines the lower limit of accessible forces, while the rupture forces of covalent bonds of a few nanonewtons define the upper limit. Reprinted with permission from ref 291. Copyright 2000, Elsevier.

Table 2. Techniques Used in Single-Molecule Force Spectroscopy

technique	force range (pN)	dynamical range	working principle
optical tweezers	0.01−200	≥1 ms	a bead with a higher refractive index than the surrounding medium is trapped in the focus of a laser beam and used as a force transducer and as a force sensor
magnetic tweezers	0.01−100	≥1 s	magnetic forces and/or torque are applied through a micrometer-sized magnetic bead, which serves as a force sensor
glass microneedles	>0.1	≥100 ms	an optical fiber is deflected perpendicular to the fiber axis and used as a force sensor
biomembrane force probe (BFP)	0.5−1000	≥1 ms	the deformation of a red blood cell, which is aspirated by a micropipet suction, is used to quantify the force acting on the blood cell
hydrodynamic techniques	>0.1	na	hydrodynamic flow or surface tension is used to exert forces directly on the sample molecules or on a bead, which serves as a force transducer
atomic force microscopy (AFM)	>3	≥10 μs	a microscopic cantilever beam with a sharp tip perpendicular to the beam serves as a force sensor

spectroscopy. Recently, even individual molecules have been used as force sensors to investigate bond-rupture forces in DNA with unprecedented accuracy.[311] A comparison of the different techniques can be found in the reviews by Merkel[17] and Clausen-Schaumann et al.[291] With the exception of hydrodynamic methods, all techniques have in common that a microscopic force sensor is displaced if a force acts upon it. Usually, an optical image of the sensor or a laser beam, which is deflected by the sensor, is used to monitor the sensor position. The techniques listed in Table 2 differ in accessible force range, dynamic range, and force resolution. Typically, the force constants of the sensors can be varied over several orders of magnitude by varying, e.g., the electromagnetic field strength or the size of the force sensor. As soon as the sensor is soft enough to ensure that the experimental noise is dominated by the thermal motion of the sensor and not by detector noise, the force resolution, i.e., the smallest detectable force F_{min}, no longer depends on the force constant of the sensor. In this case it is given by

$$F_{min} = \sqrt{4k_BTRB} \quad (4)$$

where k_B is the Boltzmann constant, T is the temperature, R is the coefficient of viscous damping, and B is the bandwidth.[312,313] In a given bandwidth, the force resolution depends only on the temperature and on viscous damping. Consequently, at a given tem-

perature, force and time resolution can only be improved by reducing the damping coefficient R, which can be achieved by reducing the size of the force sensor.

Of all of the techniques used in single-molecule force spectroscopy, AFM-[314] and glass-micro needle[315] based techniques are the ones that readily allow us to measure nanonewton forces with piconewton precision. This makes them suitable for the investigation of chemical-binding forces, which are on the order of nanonewtons. Furthermore, to discriminate short-range chemical forces, which act over only a few angstroms, from long-range surface forces, such as van der Waals forces or electrostatic forces, with decay lengths on the order of several nanometers, either spacer molecules, extremely sharp probes, like the tips used in AFM, or a combination of both are required. Therefore, AFM-based techniques have been the predominant tools for investigating chemical binding on the single-molecule level. Unless otherwise stated, all experimental studies discussed in the following pages were carried out with AFM-based instrumental setups. A comprehensive overview over AFM-based single-molecule force spectroscopy can be found in the review by Janshoff et al.[294]

3.3. Mechanical Rupture Forces of Single Chemical Bonds

3.3.1. Covalent Bonds

Two different routes have been explored to measure covalent binding forces at the single-bond level. The binding forces between surface atoms of solid-state materials have been determined by bringing the front atom of an AFM tip into close proximity with atoms of a planar surface and mapping the interatomic forces. These experiments were carried out under ultrahigh vacuum (UHV) conditions and some of them at liquid helium temperatures. In the other type of experiment, covalent forces within molecules have been determined by stretching individual polymers, until either the polymer backbone or the covalent surface anchor ruptures as a consequence of the applied tensile force. These experiments have been performed in solution and at room temperature. Both types of experiments are frequently accompanied by density functional calculations or molecular dynamics simulations.

3.3.1.1. Covalent Bonds between Surface and AFM Tip. To directly map the binding potentials and binding forces of covalent bonds at a surface with an AFM tip, one must approach the surface in a controlled way and ideally at defined positions of the surface. Otherwise, it is impossible to tell how many atoms of the tip and surface interact with each other during the experiment. This makes it necessary to overcome the mechanical instability of the AFM cantilever spring, which causes the tip to snap into the surface, if a stiff binding potential, like a chemical binding potential, act upon it. In conventional AFM setups, only the distance between the cantilever base and the substrate is controlled by the piezo actuators. Because the cantilever deflection d also contributes to the tip substrate separation, the actual tip−sample separation z_{ts} is not only a function of the piezo position but of the piezo position z_p minus the cantilever deflection d: $z_{ts} = z_p - d = z_p - F/k_C$, where F is the force acting on the tip and k_C is the cantilever spring constant, as illustrated in Figure 9. As soon as the stiffness of the interaction potential, i.e., the second derivative of the potential, exceeds the stiffness of the cantilever spring k_c, the tip will jump into contact with the surface. To accurately map binding potentials, the cantilever stiffness therefore should be larger than the stiffness of the potential under investigation. For short-range potentials, like chemical-binding potentials, this requires stiff AFM cantilevers, with spring constants on the order of 50−100 N/m.[316] However, in typical AFM setups, the use of these rather stiff cantilevers goes at the expense of an optimal force resolution, as detector noise and other noise sources become increasingly dominant for high cantilever spring constants. To overcome this problem, force feedback mechanisms, where the effective spring constant can be tuned during the experiment,[317,318] as well as dynamic modes with oscillating cantilevers, where lock-in techniques can be used to reduce the noise level, have been employed. In some cases, the experiments have also been carried out at liquid helium temperature, which reduces detector noise and other instrumental noise sources.

Jarvis et al. have used a magnetic force feedback mechanism, where the effective stiffness of the cantilever spring could be tuned during the experiment.[317] In addition, they applied a small force modulation, which allowed them to make use of a lock-in detection scheme. When the cantilever stiffness was gradually adapted and the cantilever deflection was held constant, while approaching the surface, they directly measured the stiffness of the interaction potential between a silicon AFM tip and a flat Si(111) surface under ultrahigh vacuum (UHV) conditions. From these data, they obtained the interaction force and potential energy by simple integration. This study represents one of the first attempts to directly measure chemical-binding potentials by AFM with single-bond resolution. However, as the authors point out, the forces measured are somewhat weaker and decay much slower than expected for purely covalent forces. The authors also report a site dependence of the force. As noted by the authors, van der Waals and other surface forces seem to be responsible for the long decay length. Why the maximum tensile force reported is only 0.3 nN, which is well below the 3.9 nN expected at low temperatures,[319] remains open. The paper does not give the temperature at which the experiments were carried out. However, thermal activation may play a role in the reduction of the experimentally observed binding force.[320,321]

Erlandsson et al.[318] used an electrostatic force feedback to probe the force acting between a tungsten tip and a Si(111) surface under UHV conditions and at room temperature. They report discrete force steps of around 2 and 5 nN. Despite the force feedback, the authors observe discontinuities in their approach and retract traces (Figure 10). According to the

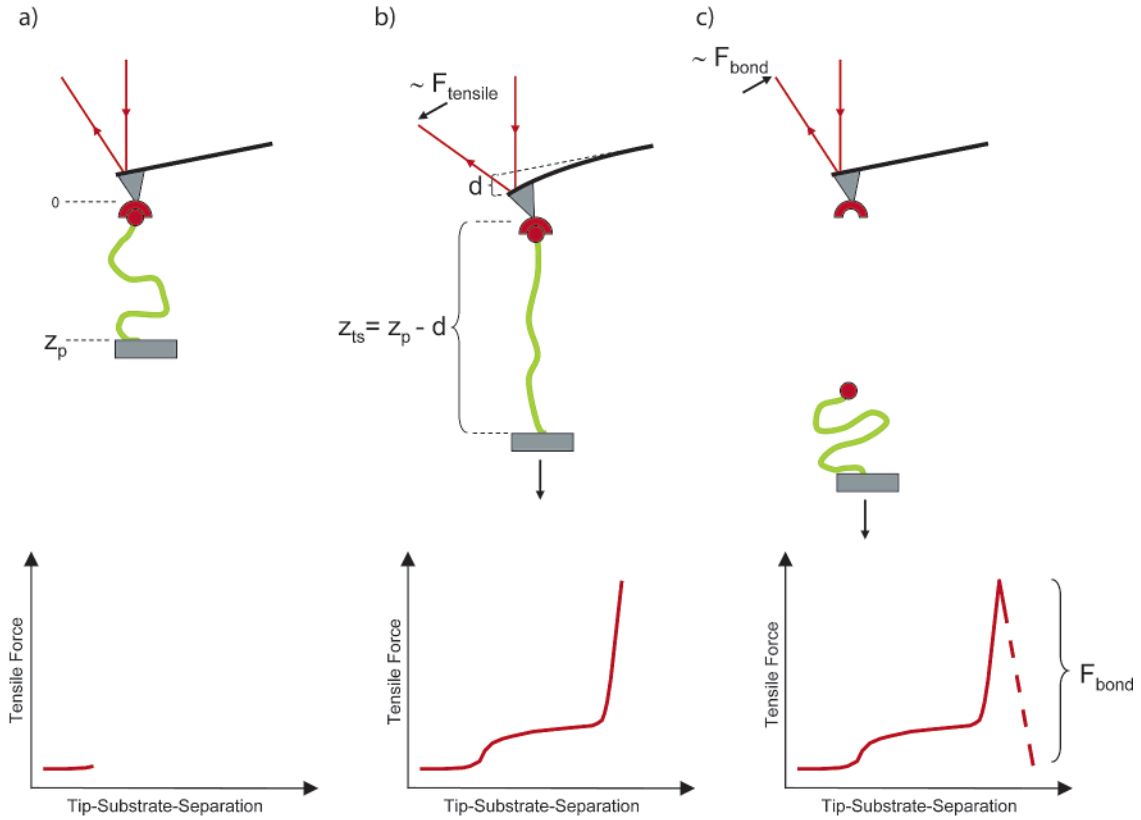

Figure 9. Schematic setup of an AFM-based force spectroscopy experiment (top) and of the corresponding force trace (bottom) of a single-molecular bond attached to a polymer tether (a). Stretching of the polymer tether reveals details of the polymer elasticity: a tensile force $F_{tensile}$ is exerted via the polymer and molecular bond to the AFM cantilever. The cantilever is displaced by a distance d, which is proportional to the exerted force, and the displacement is detected with a laser beam (b). When the tensile strength of the bond is exceeded, the molecular bond ruptures and the cantilever snaps back to its equilibrium position. The relaxation of the cantilever is proportional to the bond-rupture force F_{bond} (c).

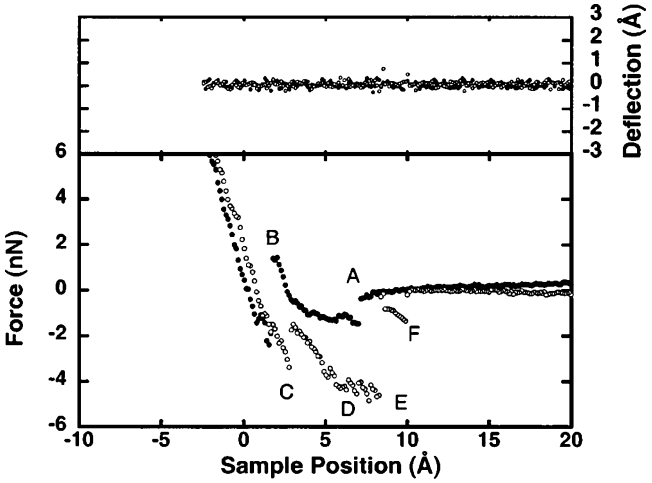

Figure 10. Cantilever deflection (top) and force (bottom) of an approach (●) and a retraction trace (○) of a W tip on a Si surface. The data were recorded using an AFM setup with an electrostatic force feedback system. The retraction trace exhibits several rupture events (C−F) and a final bond rupture of about 1.5 nN at F. Reprinted with permission from ref 318. Copyright 2000, American Physical Society.

analysis given in the paper, the force feedback is not able to fully overcome the mechanical instability when a contact is formed or a bond is broken. According to the authors, this is partially due to the finite elasticity of the tip and the surface atoms, which cannot be controlled by the feedback mechanism. The fact that no cantilever deflection is observed at the instabilities, as indicated in the upper section of Figure 10, is attributed to a slow sampling rate of the deflection signal. In their conclusion, the authors suggest that the maximum adhesive force of about 5 nN is relatively close to the theoretical value of 3.9 nN for the rupture force of a Si−Si bond.[319] However, it should be noted that, whenever chemical bonds are broken under nonequilibrium conditions and at temperatures far from absolute zero, e.g., at room temperature, a kinetic model must be used, which accounts for thermal activation of the bond-rupture process, to compare the experimental data with DFT modeling.[322−324] Because rupture forces decrease with increasing bond length,[323] it is to be expected that the rupture force of the W−Si bond is significantly lower than for the Si−Si bond. In addition, calculations by Pérez et al.[325,326] yield bond-rupture forces between 2.25 and 2.9 nN for the Si−Si bond, depending on the position of the surface atom. Thus, there are strong arguments that the measured value of 5 nN is unreasonably high. In fact, the last rupture event in the retraction trace of the force feedback data in Figure 10 shows a rupture force of about 1.5 nN, which is comparable to the tensile strength found for bonds involving metal atoms in other studies,[322,327] as discussed in detail in sections 3.3.1.2. and 3.3.2. In single-molecule force spectroscopy, it is not unusual to observe multiple bond-rupture events at the beginning of the separa-

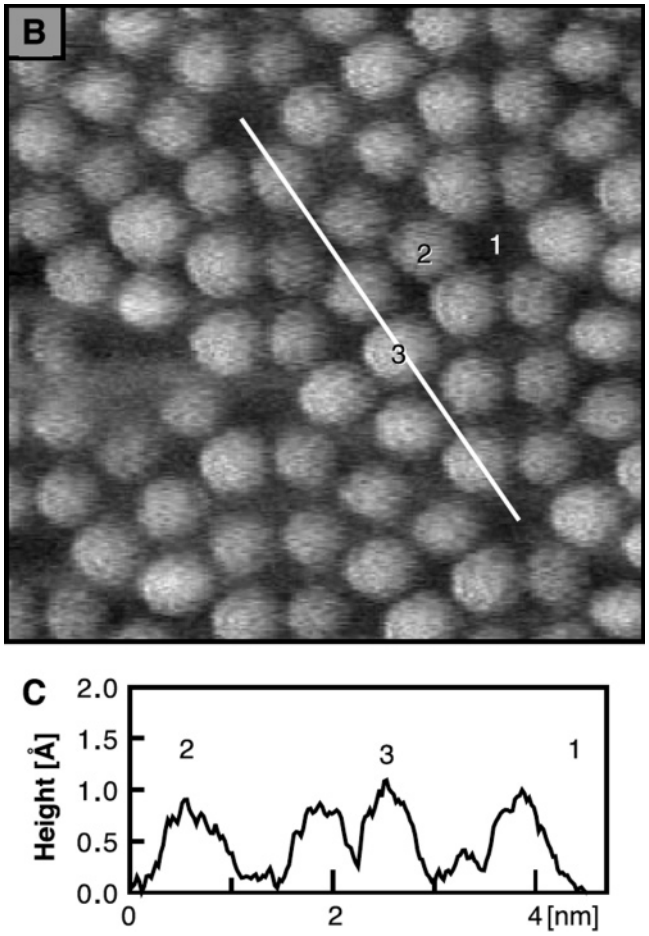

Figure 11. Topographic image of a silicon (111) 7 × 7 surface reconstruction (B) and line section (C) along the white line indicated in B. Frequency profiles were recorded at the three positions indicated, and force profiles were derived from the frequency data. Reprinted with permission from *Science* (http://www.aaas.org), ref 316. Copyright 2001, American Association for Advancement of Science.

tion process, when the initial contact between tip and surface is stretched. Often only the very last rupture event observed during the separation process actually corresponds to the breaking of a single-molecular bond. Especially for metallic bonds, initial tensile forces of a few nanonewtons and a final rupture force of about 1.5 nN have been associated with the initial stretching of several bonds in parallel and the final rupture of a single-molecular bond.[327,328] It seems therefore plausible that the final rupture event at 1.5 nN at F and possibly also the other microruptures occurring at D in the retraction trace of Figure 10 represent the failure of single covalent bonds, whereas the 5 nN steps observed correspond to the breaking of multiple bonds.

A different approach to directly map covalent binding forces between a silicon AFM tip and a Si(111) 7 × 7 surface reconstruction was pursued by Lantz and co-workers.[316,329] They used a rather stiff cantilever spring with a force constant of 48 N/m, which allowed them to avoid mechanical instabilities. Force-extension traces were recorded using a dynamic technique, where the cantilever is driven at its first resonance frequency and the shift in resonance frequency, which is induced by the tip−sample

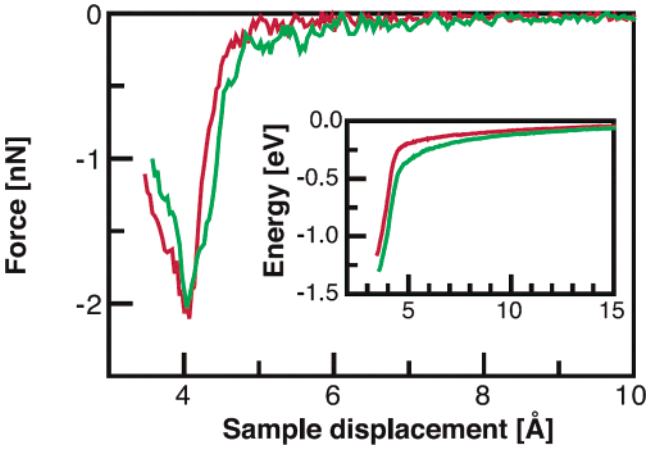

Figure 12. Short-range force and interaction energy measured above position 2 and 3 of Figure 11. Reprinted with permission from *Science* (http://www.aaas.org), ref 316. Copyright 2001, American Association for Advancement of Science.

interaction, is recorded. From this shift in resonance frequency, the force acting on the tip can then be calculated.[330−335] To reduce detector noise and instrumental drift, the experiments were carried out at 7.2 K. Before acquiring force versus distance data, Lantz et al. scanned the surface to obtain atomically resolved AFM images of the surface. While scanning, they were able to pick up a silicon atom from the surface with the cured SiO_2-covered tip, which led to an improved image contrast. They then recorded frequency versus distance traces at three defined positions of the surface shown in Figure 11: (1) a corner hole of the Si(111) 7 × 7 reconstruction, (2) a corner adatom, and (3) a central adatom. The force versus distance traces were derived from these data. The force trace above the corner hole (1), where there is no free valence at the surface that can interact with the tip, was used to quantify the long-range van der Waals force. This experimentally determined van der Waals force could then be subtracted from the forces determined at the reactive sites (2 and 3) of the surface. Furthermore, a force trace, where the tip was slightly immersed into the corner hole was used to verify that there is indeed only one dangling bond at the front atom of the AFM tip, which interacts with the surface. The force traces, illustrated in Figure 12, at the two adatom positions were then used to quantify the covalent binding forces of single Si−Si bonds. The recorded maximum tensile force was 2.1 nN (±30%) in both cases, which is in good agreement with the theoretical value of 2.25 nN predicted by Pérez et al.[325,326] Although the maximum forces are the same at both adatom positions, slight differences in the shape of the force trace can be observed, which the authors attribute to differences in chemical reactivity at the two different sites. Because of the combination of atomic resolution AFM imaging and force measurements at well-defined sites, unlike previous studies, Lantz et al. were able to attribute the observed force unambiguously to the formation and the breaking of a single covalent bond between a Si(111) 7 × 7 surface and the front atom of a Si-terminated AFM tip. It should be noted that the force values determined are expected to be

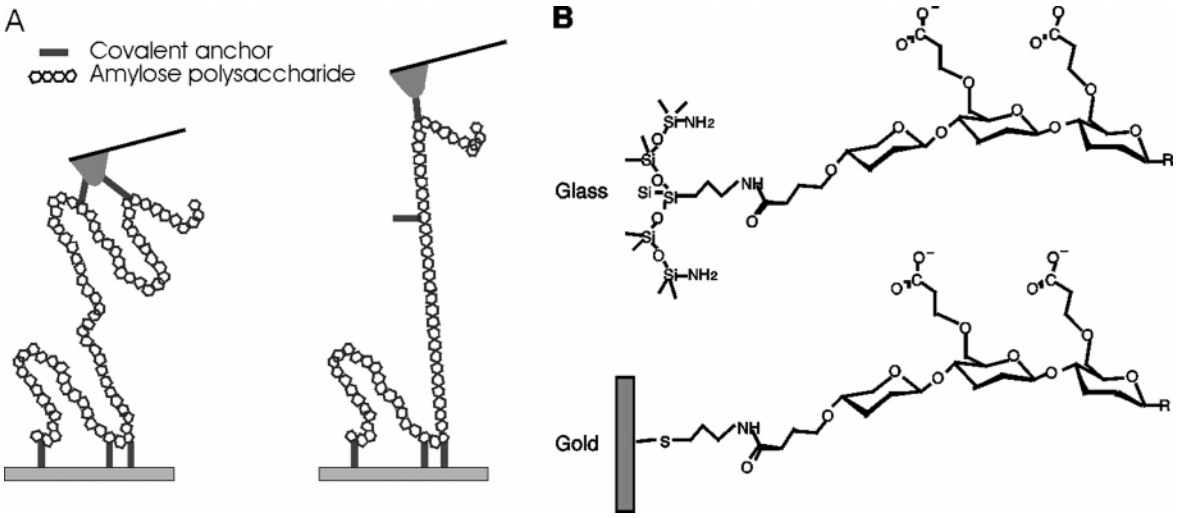

Figure 13. Carboxy-amylose polymer is covalently attached between a glass or gold substrate and an AFM tip and stretched until successive surface anchors rupture. Reprinted with permission from *Science* (http://www.aaas.org), ref 322. Copyright 1999, American Association for Advancement of Science.

independent of the kinetic parameters of the experiments, because all experiments have been conducted at temperatures close to 0 K.

With a similar strategy, Hoffmann et al. have observed short-range interaction forces between a NiO (001) surface and an NiO cluster at the end of a SiO_2-covered AFM tip.[336] They observed site-dependent short-range forces of 2.3 nN on top of a topographic surface maximum and 1.6 nN at a topographic minimum. However, in this study, the authors do not indicate which of the three possible chemical bonds, Ni−Ni, Ni−O, or O−O, is actually formed and broken during the experiments. Other studies[337−339] have investigated frequency changes and force gradients of the short-range chemical interactions of a tungsten tip with silicon surfaces at room temperature, using extremely stiff tungsten cantilever springs with $k_C > 100$ N/m and an off-resonance dynamic measuring mode. However, force values are not given.

Pérez et al.[325,326] and Buldum et al.[319] used density functional methods (DFT) based on nonlocal pseudopotentials to calculate the total energy of the tip−surface system as a function of the tip−surface distance. Their model tips are both terminated; Pérez et al. use H atoms, and Buldum et al. use another layer of Si atoms, which in turn keep unsaturated bonds. Chemically speaking, Buldum et al.'s tip is more reactive. Probably the decisive difference, however, is that Pérez et al. perform fully relaxed calculations of the surface and the tip, while Buldum et al. keep the surface and tip rigid. It has been shown that additional degrees of freedom reduce the maximum force,[323] because they allow the system to reduce its energy. Both effects together may very well account for the difference in the calculated force, 2.25 nN by Pérez et al.[325,326] versus 3.9 nN by Buldum et al.[319]

3.3.1.2. Covalent Bonds in Linear Molecules. The experiments described above deal with chemical bonds between surface atoms of extended solid-state materials, where the chemical reactivity of the atoms is affected by the electronic band structure of the solid and where the forces depend on the lateral position on the surface. For atoms in molecules, the situation is somewhat different. Here, the electronic wave functions of two atoms interact with each other to form a covalent bond. These studies are usually conducted in solvent and at room temperature, and the tensile force is gradually built up along the backbone of extended polymeric molecules. The AFM tip and substrate surface are therefore separated by tens or even hundreds of nanometers before the force actually reaches a level that is sufficient to break chemical bonds. At these distances, long-range van der Waals and electrostatic forces no longer act between the AFM tip and substrate surface and thus no longer interfere with the short-range chemical forces investigated. If ions are present in the solvent, electrostatic forces are also screened within a few nanometers.[271]

In an early attempt to quantify the covalent binding forces within molecules, Bensimon and coworkers have used a receding water meniscus to stretch and rupture individual DNA molecules, which were attached on both ends to a functionalized glass surface.[340] They estimated the forces required to rupture the backbone of double-stranded DNA by analyzing the deformations of the ruptured molecules and comparing them to the bending energy of DNA. Their value for the maximum tensile force in double-stranded DNA was 476 pN. However, in light of later findings, where DNA has been stretched with forces of more than 800 pN without rupturing,[341] this value seems to be rather low.

Grandbois et al.[322] have determined covalent binding forces in molecules by stretching individual carboxy-amylose polymers, which were covalently attached between a functionalized glass surface and an AFM tip, depicted in Figure 13. In a first step, carboxy-amylose was activated with ethyl-dimethyl-aminopropyl-carbodiimide (EDC) and *N*-hydroxy-succinimide (NHS) and incubated onto an amino-functionalized glass surface. After the surface was rinsed to remove noncovalently bound molecules, an amino-functionalized AFM tip was lowered toward

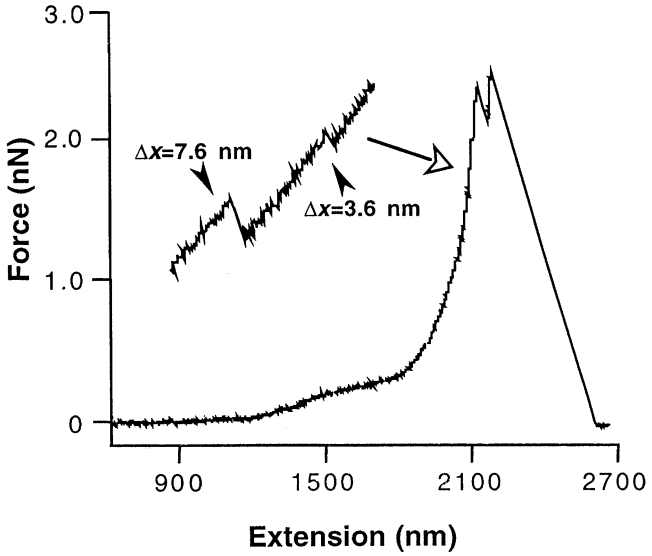

Figure 14. Force extension profile of carboxy-amylose attached to an amino-silanized glass surface. At forces near 2 nN, microruptures, which correspond to the rupturing of successive surface anchors, can be observed (inset), until the connection between the AFM tip and substrate surface is finally lost at a force of about 2.5 nN. Reprinted with permission from *Science* (http://www.aaas.org), ref 322. Copyright 1999, American Association for Advancement of Science.

the substrate surface to couple individual polysaccharide strands to the AFM tip. To avoid the attachment of multiple strands, the authors made use of the so-called "fly-fishing mode",[275] lowering the tip stepwise and partially retracting it after each approach, until a single binding event was observed upon pulling the tip back. The authors also checked their force extension profiles for scalability, which is a well-known criterion for stretching single molecules. The force profiles of carboxy-amylose exhibit a pronounced plateau at 275 pN, which is caused by a chair−boat transition of the furanose rings.[342−345] In the case of multiple attachments, this plateau is either shifted to higher forces or smeared out. Whenever a single polymer was covalently attached between the AFM tip and the substrate surface, the polymer was stretched, until the connection between the AFM tip and the glass surface ruptured. The rupture of these single-molecule bridges occurred in multiple irreversible steps: several microruptures occurred, before the connection between the tip and substrate was finally lost. Figure 14 shows a typical force-extension profile of the carboxy-amylose experiment on glass.[322] The length increase of the polysaccharide chain after each microrupture corresponded to multiples of the carboxy-amylose monomer length, indicating that successive covalent surface anchors had failed, before the molecule was finally detached. At the applied force-loading rate of 10 nN/s, the authors observed an average bond-rupture force of 2.0 ± 0.3 nN, while in control experiments with no EDC or NHS added, the mean bond-rupture force was below 1 nN, as illustrated in Figure 15. This is consistent with other studies where polysaccharides have been nonspecifically attached between the AFM tip and substrate surface.[275,342,343]

To find out which of the chemical bonds of the surface anchor actually ruptured in the experiments, Grandbois et al. compared this value with the results of theoretical calculations based on the DFT.[322,323] It is important to note that a direct comparison of experimental values to DFT results is not possible, because the experiments were carried out at room temperature. Here, thermal activation of the bond-rupture process has to be considered, and the experimentally observed rupture forces are a function of the temperature and of the rate dF/dt, at which the external force is applied. Therefore, a convolution of the modified Arrhenius rate law (2) with the experimental force-loading rate has to be used to calculate the bond-rupture probability densities as a function of the applied force. The binding potentials, which were derived from DFT calculations, were used to determine the force-dependent activation barrier E_A, which enters the Arrhenius function.

The bond-rupture probability densities, which had been derived in this fashion from the DFT calculations, clearly indicated that the Si−C bond, which is localized in the surface anchor, was the weakest of all of the bonds that were loaded in the experiments. Nevertheless, the theoretical value of 2.7 nN for the Si−C bond is slightly higher than the experimentally observed value of 2.0 ± 0.3 nN. This is explained by the authors with solvent effects, which were not considered in the DFT calculations. The effect of solvent molecules and ion concentrations in the buffer

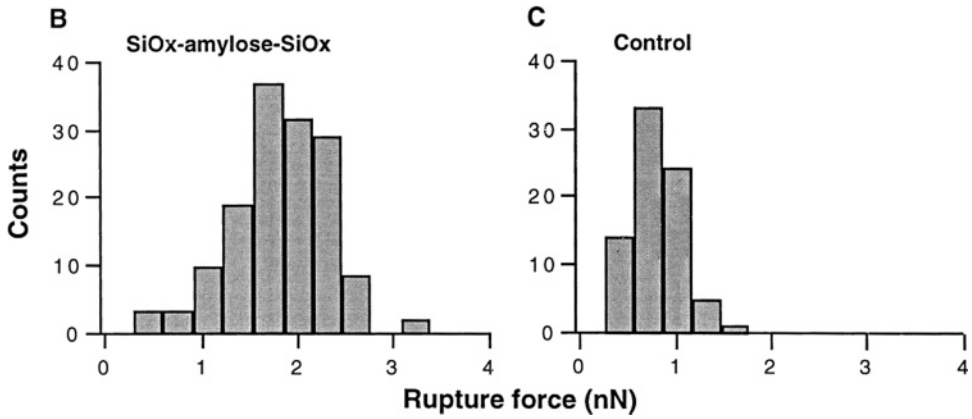

Figure 15. Distribution of bond-rupture forces observed (B) for covalently attached carboxy-amylose and (C) in control experiments, where no cross-linking agent (EDC/NHS) was added. Reprinted with permission from *Science* (http://www.aaas.org), ref 322. Copyright 1999, American Association for Advancement of Science.

solution on strained chemical bonds is indeed still poorly understood and should be systematically addressed in future studies. Another explanation might be that a constant force-loading rate of 10 nN/m was convoluted with the Arrhenius rate function, to derive the theoretical value of 2.7 nN. However, because of the nonlinear compliance of the polysaccharide chain, this corresponds to the actual experimental loading rate only for relatively high forces, close to the final bond-rupture force. Recent theoretical studies[346,347] indicate that, when polymeric spacer molecules with a nonlinear force response are used in bond-rupture experiments, thermally activated bond ruptures at smaller forces and thus smaller force-loading rates already contribute to the measured bond-rupture probabilities and shift the experimentally observed mean bond-rupture forces toward slightly smaller values, compared to values which would be obtained for a truly linear system with a constant force-loading rate. As a consequence, the time dependence of dF/dt should be considered in the convolution with the Arrhenius rate function, when comparing experimental data with theoretical modeling.

In addition to the amino-silane coupling to a glass surface, Grandbois et al. also used amino-thiols, attached to a gold surface, to immobilize the carboxyamylose, while the attachment to the AFM tip remained unchanged. In these experiments, the mean bond-rupture force was shifted to 1.4 ± 0.3 nN, indicating that the surface attachment was again the weakest link in the chain. Because the authors do not provide a theoretical estimate for the S−Au and the Au−Au bonds, it remained open which bond actually ruptures in this case. This problem was addressed in a series of theoretical publications by Krüger et al., using static DFT calculations as well as quantum molecular dynamics (Car−Parrinello) simulations.[11,348,349] Their results clearly indicate that pulling the thiolate molecule on a stepped gold surface leads to the formation of a monatomic gold nanowire,[11,349] followed by breaking a Au−Au bond with a rupture force of about 1.2 nN.[349] It is of course quite tempting to directly compare their value with the experimentally measured 1.4 ± 0.3 nN.[322] However, the simulation is done on a 200 ps time scale and in a vacuum, while the experiments proceed on a time scale of 1 s and in solution. The simulations show that, prior to bond rupture, the actual pulling of the nanowire requires forces of up to 2.1 nN.[349] Probably, this is the process that is actually probed in the experiment, with the different time scales and possibly solvent effects lowering the peak force in the sequence of events from 2.1 to 1.4 nN. The final bond-rupture event, which according to the calculation is expected at 1.2 nN, i.e., in the experiments for similar reasons probably well below 1.0 nN, cannot be detected in the experiment because of the dynamic instability of the AFM tip. Again, probably fortuitously, the experimental Au-thiole value compares favorably with the Au−Au rupture force of 1.5 nN measured at 4.2 K by Rubio-Bollinger et al.[328]

In the experiments by Grandbois et al., values for the covalent bond-rupture forces at a force-loading rate of 10 nN/s have been determined. However, because of the mechanical instabilities of the AFM cantilever and the tethered polymer, the lever and polymer snap back immediately, after the connection between the tip and substrate surface is lost. Because of the "blind window" caused by this snapping, the exact shape of the binding potential cannot be assessed in these experiments. To obtain structural information on the binding potential, like potential depth and width, the force-loading rate must be varied systematically. A plot of mean bond-rupture forces $\langle F \rangle$ versus the logarithm of the force-loading rate $\ln(dF/dt)$ then reveals these structural parameters in a straightforward manner.[321,350]

Garnier et al.[351] have chosen an alternative approach and used a magnetic force feedback system to overcome the mechanical instability of the cantilever. To avoid a snapping of the tethered polymer, the authors used short polymeric spacers with a high intrinsic stiffness: approximately 10 nm long PMAA spacers with thiol groups on both ends were stretched between a gold-coated AFM tip and a gold substrate. The authors observed a maximum tensile force of 2.2−2.9 nN, which is comparable to the theoretical values for the Au−S and the Au−Au bonds obtained from their DFT calculations. In these calculations, they also obtained values for the strength of C−C and C−S bonds, which are comparable to the F_{max} values obtained by Beyer for C−C and C−Si, respectively, as listed in Table 4.[323] Interestingly, a comparable value of 5.64 nN for the C−C bond was already obtained in 1936 by de Boer,[352] who calculated the maximum slope of a Morse potential. However, because the role of kinetic effects and thermal activation is not addressed by Garnier et al. and neither force-loading rate nor piezo velocity is given, it is difficult to compare these results to other studies. It should also be noted that the force resolution of the magnetic force feedback system is only 0.5 nN, compared to 0.01 nN and better for conventional AFM setups.

3.3.2. Metallic Bonds—Gold Nanowires

Nanowires of various materials have been extensively studied in the past decade,[353−368] and it is well-established both experimentally and theoretically that gold nanowires with a diameter of a single atom form upon pulling a gold nanojunction. Gold nanowires can be considered as a prototype system of nanoscale mechanochemistry. The mechanical strength of single-atom metallic contacts in such gold nanowires has been determined both at room temperature and 4.2 K by Rubio et al.[327,328] In these studies, the authors pulled gold nanowires out of a gold surface by retracting a gold tip, which previously had been brought into contact with a gold surface. To monitor the diameter of the contact, the authors measured the electronic conductance of the nanowire and the tensile force simultaneously, as the gold nanowire was elongated. The fact that the conductance of a single gold atom or a wire with the diameter of one atom is close to the quantum unit of conductance $2e^2/h$, where e is the elementary charge and h is Planck's constant, makes it possible to infer the diameter of the nanocontact from its conductance. Each additional atom in the diameter adds ap-

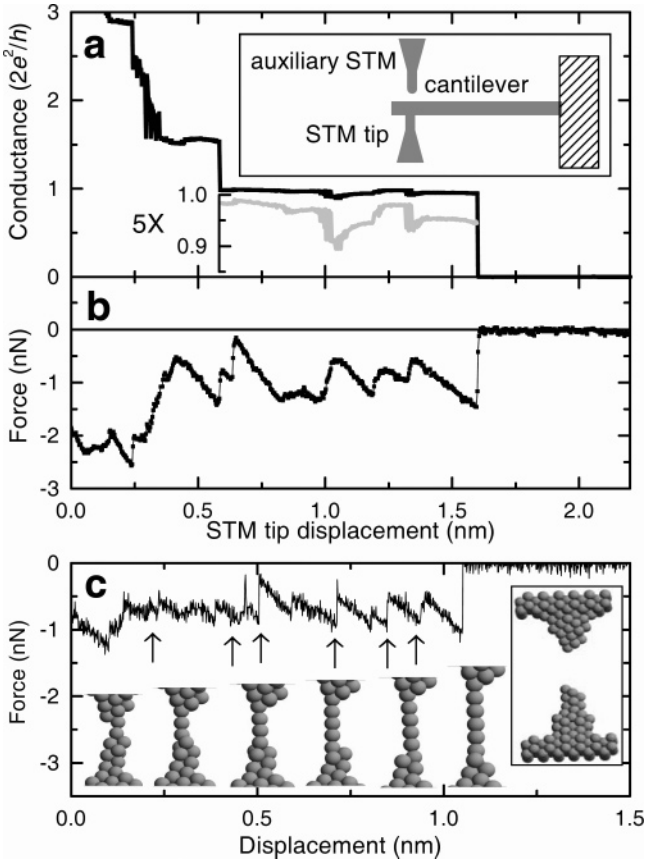

Figure 16. Experimental setup (inset) and conductance versus extension curve of the stretching of a single atom metallic junction (a). Force versus extension curve of the same single atom metallic contact (b) and calculated force and snapshots of the MD simulation of a simulated rupture of a metallic contact (c). Reprinted with permission from ref 328. Copyright 2001, American Physical Society.

proximately $2e^2/h$ to the conductance. The experimental setup consisted of a microscopic gold wire, which was mounted between two scanning tunneling microscope (STM) tips. One STM tip was used to form and stretch the metallic contact and measure the electronic conductance, while the second auxiliary tip was used to monitor the displacement of the microscopic gold wire, which served as a gold substrate and at the same time was used as a cantilever force sensor (Figure 16a). During elongation of the gold nanowire, the tensile force dropped in a discrete stepwise fashion whenever the diameter of the contact was reduced by a discrete number of atoms, until the contact diameter was reduced to one single atom (Figure 16b). Upon further elongation, a wire with a diameter of one gold atom was pulled out of the surface, and whenever an additional gold atom was incorporated into the wire, again, a step could be observed in the force curves, until the gold nanowire finally ruptured. Both, the room temperature and the liquid helium temperature experiments exhibited a rupture force of 1.5 nN. In the case of the 4.2 K experiments, more than 200 final rupture events were evaluated. The result is a force distribution with a mean value of 1.5 ± 0.3 nN, at a pulling velocity of 0.5 nm/s. Why the rupture force is the same, both for the room temperature experiments, where thermal activation is expected to reduce the observed bond-rupture force, and for the 4.2 K experiments, where thermal activation should be negligible, remains open. The experimental findings at low temperature have been corroborated by molecular dynamics simulations at 4 K and by DFT calculations (Figure 16c). Interestingly, according to the DFT calculations, the tensile strength of a single Au−Au bond is about 2 times higher for 2-fold coordinated gold atoms in a nanowire than the tensile strength of Au−Au bonds in bulk material, where the coordination is considerably higher. This mechanical strengthening of metallic bonds with reduced coordination is in fact responsible for the experimentally observed formation of a single-atom diameter gold nanowire, upon pulling apart the Au−Au contact.

In a recent study,[369] Rubio-Bollinger et al. have investigated the interaction potential between single gold atoms in more detail, by measuring force gradients, using a dynamic mode and rather stiff force sensors, with force constants $k_C \cong 2$ kN/m. Again, the electrical conductance was monitored simultaneously. Although these force sensors did not show mechanical instabilities at the contact point, there is a jump into contact occurring over the last angstrom, which is attributed to the elastics and yielding properties of the junction itself. Nevertheless, despite this small instability, the authors are able to separate the short-range metallic forces from long-range van der Waals forces. When their data were compared to theoretical modeling, detailed structural information, like binding energy, shape, and range of the potential, could be extracted. As predicted by theoretical arguments,[370] the decay length of the metallic interaction has been determined to be 5−6 Å, which is close to the Thomas−Fermi screening length of gold of 5.4 Å.

Tables 3 and 4 summarize the available experimental and theoretical results of covalent and metallic bond-rupture forces, together with the conditions or the model with which they have been obtained.

3.3.3. Coordinative Bonds—Organometallic Bonds

Similar to covalent and metallic bonds where the electronic wave functions of the binding partners overlap and electrons are shared between the partners, coordinative bonds, like those found in organometallic complexes, are formed by partially overlapping electronic wave functions. Usually more than two atoms are involved, and therefore, geometric constraints play a crucial role in the bond formation. Changing the electronic configuration of one of the binding partners, e.g., by changing the ionization state of a metal ion, usually has a marked effect on the strength of the bond.

The first coordinative organometallic bond studied using single-molecule force spectroscopy, was the *N*-nitrilo-triacetic acid (NTA)/histidine (His)-tag system, which is widely used in molecular biology and biotechnology for the purification and screening of recombinant proteins. The tetrahedal ligand NTA forms a hexagonal complex with divalent metal ions, such as Ni^{2+}, Co^{2+}, Cu^{2+}, or Zn^{2+}, occupying four of the six binding sites. The remaining two binding sites are accessible to the electron-donating amino acid

Table 3. Experimental Values of Covalent and Metallic Bond-Rupture Forces

bond	rupture force (nN)	force-loading rate (nN/s)	temperature (K)	experimental conditions	author
C−C	2.6−13.4	na	room temp.	elongational flow	Odell et al.[52]
Au−Au	1.5 ± 0.3		4.2	gold nanowire	Rubio-Bollinger et al.[328]
Au−Au	1.5 ± 0.2		room temp.	gold nanowire	Rubio et al.[327]
Au−Au (or Au−S)	1.4 ± 0.3	10	room temp.	alkane-thiol on Au surface in buffer solution (pH 7.4)	Grandbois et al.[322]
Au−Au (or Au−S)	2.2−2.9			alkane-thiol on Au surface	Garnier et al.[351]
C−Si	2.0 ± 0.3	10	room temp.	silane on glass in buffer solution (pH 7.4)	Grandbois et al.[322]
Si−Si	2.1 ± 0.3		7.2	bond between two surface atoms; UHV	Lantz et al.[316]

Table 4. Theoretical Values of Covalent and Metallic Bond-Rupture Forces

bond	rupture force (nN)	convoluted force-loading rate (nN/s)	temperature (K)	method	author
Au−Au	1.55−1.68			DFT	Rubio-Bollinger et al.[328]
Au−Au	about 1.2		4	MD (EMT)	Rubio-Bollinger et al.[328]
Au−Au	2.5			DFT/ZORA[a]	Garnier et al.[351]
Au−S	2.7			DFT/ZORA[a]	Garnier et al.[351]
C−C	5.64			empirical Morse potential	de Boer[352]
C−C	6.0			DFT	Garnier et al.[351]
C−S	3.7			DFT	Garnier et al.[351]
C−C	6.9			DFT	Beyer[323]
C−Si	2.8 ± 0.1	10	298	DFT	Grandbois et al.[322]
Si−Si	2.25			DFT	Pérez et al.[325,326]
Si−Si	3.9			DFT	Buldum et al.[319]

[a] Includes relativistic corrections.

Table 5. Experimental Values of NTA/His-Tag Bond-Rupture Forces

bond	rupture force (pN)	force-loading rate (nN/s)	experimental conditions	author
NTA−Co^{2+}−His_6	22 ± 4		C-terminal His tag (piezo velocity, 0.5 μm/s)	Schmitt et al.[372]
NTA−Cu^{2+}−His_6	58 ± 5		C-terminal His tag (piezo velocity, 0.5 μm/s)	Schmitt et al.[372]
NTA−Ni^{2+}−His_2	300		C-terminal His tag (piezo velocity, 1 μm/s)	Conti et al.[371]
NTA−Ni^{2+}−His_6	500		C-terminal His tag (piezo velocity, 1 μm/s)	Conti et al.[371]
NTA−Ni^{2+}−His_6	150 ± 38	4.5	N-terminal His tag	Kienberger et al.[373]
NTA−Ni^{2+}−His_6	188 ± 64	43	N-terminal His tag	Kienberger et al.[373]
NTA−Ni^{2+}−His_6	194 ± 83	70	N-terminal His tag	Kienberger et al.[373]
NTA−Ni^{2+}−His_6	38 ± 4		C-terminal His tag (piezo velocity, 0.5 μm/s)	Schmitt et al.[372]
NTA−Zn^{2+}−His_6	28 ± 3		C-terminal His tag (piezo velocity, 0.5 μm/s)	Schmitt et al.[372]

side groups of the His tag. A minimum of two histidines are necessary to form a stable bond; however, typically a His tag consists of five or six consecutive histidines. In three independent, parallel studies, Conti et al.,[371] Schmitt et al.,[372] and Kienberger et al.[373] have determined the binding force of a single NTA/His-tag bond. In all three studies, either the NTA ligand or the His tag was attached to a polymer spacer to avoid short-range surface forces. Conti et al. and Schmitt et al. used a commercially available chip with a dextrane−NTA conjugate as a substrate and attached a polypeptide chain with a C-terminal His tag to the AFM tip, [371,372] while Kienberger et al. used an N-terminal poly(ethylene glycol) His-tag conjugate on the tip and a thiol-NTA on the substrate surface.[373] Kienberger et al. and Schmitt et al. used six consecutive histidines (His_6), while Conti et al. investigated both His_2- and His_6-tagged proteins. Finally, Schmitt et al. investigated bond-rupture forces for four different divalent metal ions, while the other studies were restricted to Ni^{2+}. The results are summarized in Table 5.

For the NTA−Ni^{2+}−His_6 system, which has been investigated in all three studies, forces ranging from 38 to 500 pN have been reported. Kienberger et al. have pointed out that the fact that they used an N-terminal His tag may explain the reduced bond-rupture forces, compared to Conti et al., who used a C-terminal His tag. However, in light of the results of Schmitt et al., this explanation seems questionable. Unlike Kienberger et al., who determined the bond-rupture force of the NTA−Ni^{2+}−His_6 complex for three different force-loading rates, the other authors do not give a force-loading rate for their experiments. Although the piezo velocities are given, a direct comparison between the different results is not possible, because the combined elasticity of spacer molecules and cantilever spring, which would allow a calculation of the force-loading rates, is not known. Because Kienberger et al. determined the bond-rupture forces for three different force-loading rates, they were also able to extract lifetime and structural information from their data, using the relationship

$$F^* = \frac{k_B T}{x_b} \ln \frac{x_b (dF/dt)}{\nu_0 k_B T} = \frac{k_B T}{x_b} \ln \frac{\tau_0 x_b (dF/dt)}{k_B T} \quad (5)$$

where F^* is the most probable unbinding force, ν_0 is the off-rate, τ_0 is the bond lifetime without an external force, x_b is the bond length, and dF/dt is the

Table 6. Experimental Values of Coordinative Bond-Rupture Forces

bond	rupture force (pN)	force-loading rate (nN/s)	remarks	author
18-crown-6 ammonium	60		force determined only indirectly from peaks in the force distribution	Kado et al.[374]
β-cyclodextrin ferrocene	55 ± 10	$2-10^3$	no loading rate dependence	Zapotoczny et al.[375]
β-cyclodextrin anilylthiol	39 ± 15	$2-10^3$	no loading rate dependence	Auletta et al.[377]
β-cyclodextrin toluidylthiol	45 ± 15	$2-10^3$	no loading rate dependence	Auletta et al.[377]
β-cyclodextrin *tert*-butylphenylthiol	89 ± 15	$2-10^3$	no loading rate dependence	Auletta et al.[377]
β-cyclodextrin adamantylthiol	102 ± 15	$2-10^3$	no loading rate dependence	Auletta et al.[377]
terpyridine$-Ru^{2+}$ terpyridine	95	1	centrally attached spacer	Kudera et al.[381]

rate at which the force is applied. Using τ_0 and x_b as fit parameters gave a bond lifetime τ_0 of 15 s and an effective bond length x_b of 1.9 nm.

Other coordinative and organometallic bonds studied by single-molecule force spectroscopy include the 18-crown-6 ammonium, the β-cyclodextrin ferrocene, and the terpyridine rubidium systems. The 18-crown-6 ammonium bond-rupture force has been determined indirectly by Kado et al.[374] Although the authors do not observe single-bond-rupture events in their force traces, distinct peaks at multiples of 60 pN are found in the distribution of the observed bond-rupture forces and in the autocorrelation function of this distribution.

Like the crown ethers, β-cyclodextrin is a cyclic macromolecule, which forms a stable complex with the organometallic ferrocene molecule, as well as a number of other ligands. The mechanical strength of the β-cyclodextrin ferrocene system has been determined by Vancso and co-workers, who coupled ferrocene-alcane-thiol conjugates of different alcane chain lengths to a gold-coated AFM tip and brought them into contact with a self-assembled monolayer of β-cyclodextrin host complexes.[375,376] For both spacer molecules, the authors observed bond-rupture forces at 55 ± 10 pN, and the distribution of bond-rupture forces shows distinct maxima at 55 pN and at multiples thereof. Interestingly, although the authors varied the force-loading rate over almost 3 orders of magnitude, from 2 to 10^3 nN/s, they did not observe a loading rate dependence of the bond-rupture force. This observation is explained by the authors with the extremely fast kinetics of this system, with rate constants for the on and off reactions that are much faster than the accessible time scales in AFM experiments. A study from the same lab, in which the bond-rupture forces of four other ligands bound to β-cyclodextrin[377] were systematically investigated, further corroborated this finding: for all four ligands, the bond-rupture forces were independent of the force-loading rate, as summarized in Table 6. Furthermore, the bond-rupture forces followed the same trend as the Gibbs free enthalpies, which, according to the authors, is an indication that the dissociation process occurs near thermodynamic equilibrium. However, it should be noted that, for a truly adiabatic process, force curves should be fully reversible, with no snapping of the cantilever upon bond separation. This is the case, e.g., for the mechanical separation of long DNA double strands, where the connection between two strands is not lost when a base pair opens.[280,341,378,379] In such a case, the bonds between individual bases can open and close many times in the course of an experiment, and the Gibbs free enthalpy can be obtained by simple integration of the force extension curve.

2,2′:6″,2″-Terpyridine is a widely used ligand in supramolecular chemistry, which forms numerous transition-metal complexes and is used to build defined block copolymers of AB, ABA, or ABC form.[380] In the presence of divalent metal ions, such as Co^{2+}, Zn^{2+}, or Ru^{2+}, 2,2′:6″,2″-terpyridine forms a stable bisterpyridine complex. To determine the bond-rupture forces for the bisterpyridine$-Ru^{2+}$ complex, Kudera et al.[381] attached a poly(ethylene oxide) spacer to the 4-C atom of the central pyridine ring and immobilized the polymeric spacers on amino-functionalized glass surface and on the amino-functionalized AFM tip via their carboxyl end groups. To avoid complex formation between terpyridines of the tip or of the substrate surface, in a first step, the authors formed defined monocomplexes of terpyridine with Ru^{3+} at the substrate surface, followed by *in situ* reduction of Ru^{3+} to Ru^{2+}. At a force-loading rate of 1 nN/s, the bond-rupture force was found to be 95 pN. Variation of the force-loading rate over more than 1 order of magnitude also yielded the kinetic and structural parameters of the bond. The dissociation rate at zero force ($\nu_0 = 1/\tau_0$) was estimated to be 0.02 s^{-1}, and the bond length x_b was 3 Å.

3.3.4. Charge-Transfer Complexes

The last type of chemical interactions discussed in this part of the review is the binding of charge-transfer complexes of electron donors and electron acceptors. Here again, electronic wave functions overlap, and electrons are shared between two molecules to form a distinct chemical bond. Skulason and Frisbie determined the bond-rupture forces for derivatives of the well-known electron donor *N*,*N*,*N*′,*N*′-tetramethylphenylenediamine (TMPD) and the electron acceptor 7,7,8,8-tetracyanoquinodimethane (TCNQ), which were immobilized on Au-coated AFM tips and substrates via S$-$Au chemistry.[382] By selecting appropriate surface groups and solvents, the authors were able to minimize the nonspecific interaction between the tip and surface caused by surface tension. The observed distribution of bond-rupture forces shows distinct peaks at a force of 70 ± 15 pN and at multiples thereof. This finding is also reflected by the autocorrelation function of the rupture force distribution and by Fourier transform of the autocorrelation function. In various blocking and other control experiments performed by the authors, no distinct intervals can be observed in the force distribution and the total number of binding events, as well as the mean rupture force, is significantly reduced. A comparison of binding enthalpies with the

mechanical energy necessary to rupture the bond as well as the asymmetric attachment of the spacer molecules lead the authors to the conclusion that a sliding mechanism is the most likely path of mechanical bond separation. Interestingly, here again, the authors observed no change in the bond-rupture forces as they varied the pulling velocity over 1 order of magnitude. Why this is the case remains open.

However, it should be noted that, in the studies where no force-loading rate dependence of the rupture force was observed,[375−377] the single-bond-rupture forces were derived from periodicities in the rupture force distribution. In both experiments, the majority of events observed were simultaneous ruptures of multiple bonds, rather than single-bond-rupture events. A theoretical investigation by Seifert[383] shows that, for the mechanical failure of multiple bonds in parallel, the observed bond-rupture force does not necessarily increase monotonically with the applied force-loading rate. Even for single-molecular bonds, there is only a logarithmic dependence of the observed bond-rupture force on the force-loading rate, and especially for wide-binding potentials, the variation in the observed rupture force is small, if the force-loading rate is varied.

3.4. Knotted Polymers

It is well-known that knotted macroscopic ropes or fishing line break right at the knot.[384] On the single-molecule level, it is equally well-established that long polymer chains contain knots.[385] In the context of mechanochemistry, this immediately raises the question whether a knotted polymer behaves similarly to a macroscopic rope, i.e., will it also break at the knot and to what extent is the rupture force lowered? Arai et al.[386] succeeded to tie individual DNA and actin filaments into a knot, using optical tweezers. The actin filament breaks at a force of 1 pN, which is 2 orders of magnitude smaller than the tensile stress of a straight filament.[387] The DNA molecule was found to be stronger than the actin filament. With the low forces exerted by molecular tweezers, the DNA molecule did not break. Bao et al.[388] repeated the knotting of individual DNA molecules, again using molecular tweezers, and studied the mobility of the knots along the molecule. They found that the knots are mobile and diffuse thermally, with classical random walk statistics.

Saitta and Klein[389,390] conducted quantum molecular dynamics simulations of a knotted polyethylene chain and found that indeed also this prototype polymer ruptures at the entrance to the knot, with a homolytic C−C bond cleavage. The strain energy per C−C bond at the breaking point was 53.1 kJ mol^{-1}, compared to 67.8 kJ mol^{-1} for an unknotted chain, illustrating the weakening of the polymer. Investigating the fate of the mechanoradicals generated in the chain scission, the same authors identify typical secondary reactions: recombination, formation of cyclic alkanes, and disproportionation phenomena with nearby chain segments.[391] Studies designed to model bulklike behavior confirmed these results.[392,393] In a simulation of a fiber extrusion process, the knot was found to nucleate crystallization of the sample on a nanosecond time scale.[394] Recently, unknotting of a polymer strand in a melt was studied by Kim and Klein.[395] Monte Carlo simulations have been conducted by Kardar and co-workers.[396,397] They found that tight knots in open polymers are removed by diffusion along the chain, rather than by opening up.

3.5. Theoretical Studies: Beyond Homolytic Bond Cleavage

The AFM experiment by Grandbois et al.[322] was accompanied by theoretical modeling, which was described in detail in a later publication.[323] In this work, small model molecules were stretched in relaxed potential-energy surface scans, yielding the total energy of the molecule as a function of length. Because this approach is universally taken by all researchers using theoretical calculations,[319,324−326,351] the term COGEF potential was suggested for this function, for constrained geometries simulated external force.[323] When these COGEF potentials were coupled with the kinetic model described above, they yielded a number of generally applicable results. Chemists are used to thinking of bond strength in terms of energy, and accordingly, one would expect that rupture forces are correlated mainly with the dissociation energy of the bond. However, because the force is the energy change per unit length extension, it turns out that bond length is actually more important than bond energy. As a rule of thumb, rupture forces decrease with increasing bond length, i.e., with increasing radius of the atoms. A similar trend has been observed in the early days of spectroscopy for the bond-force constants of diatomic molecules,[398] illustrating the conceptual connection between the force constant and rupture force. Another aspect found in these model calculations was that additional degrees of freedom in the molecule lower the rupture force.

Kinetic modeling was undertaken, adapting the approach of Kauzmann and Eyring.[38] Figure 17 shows a Morse potential, which is deformed by the presence of an external force. For the quantitative evaluation based on DFT calculations, the Morse potential parameters β and D_e are extracted from the COGEF potentials, which yield directly F_{max} and D_e, using relations similar to those derived by Plotnikov for the photodegradation of stressed polymers:[261]

$$V = D_e(1 - \exp(-\beta x))^2 \quad (6)$$

$$\beta = 2F_{max}/D_e \quad (7)$$

From the deformed Morse potential $V_{eff} = V - rF$, the barrier height D′ in Figure 17 is calculated as a function of force F.[323] Analogous to the Zhurkov eq 2 for bulk solids, an Arrhenius equation with D′ as activation energy yields bond dissociation rate constants as a function of the external force. Conversely, these can be used to calculate the rupture force as a function of the lifetime τ of the bond. Table 7 summarizes the results for five different lifetime time scales, ranging from 1 ps to 10^{12} s. Evidently, immediate bond rupture requires 2−3 times the force compared with a lifetime of days. On the other hand, bonds are basically indefinitely stable at still rela-

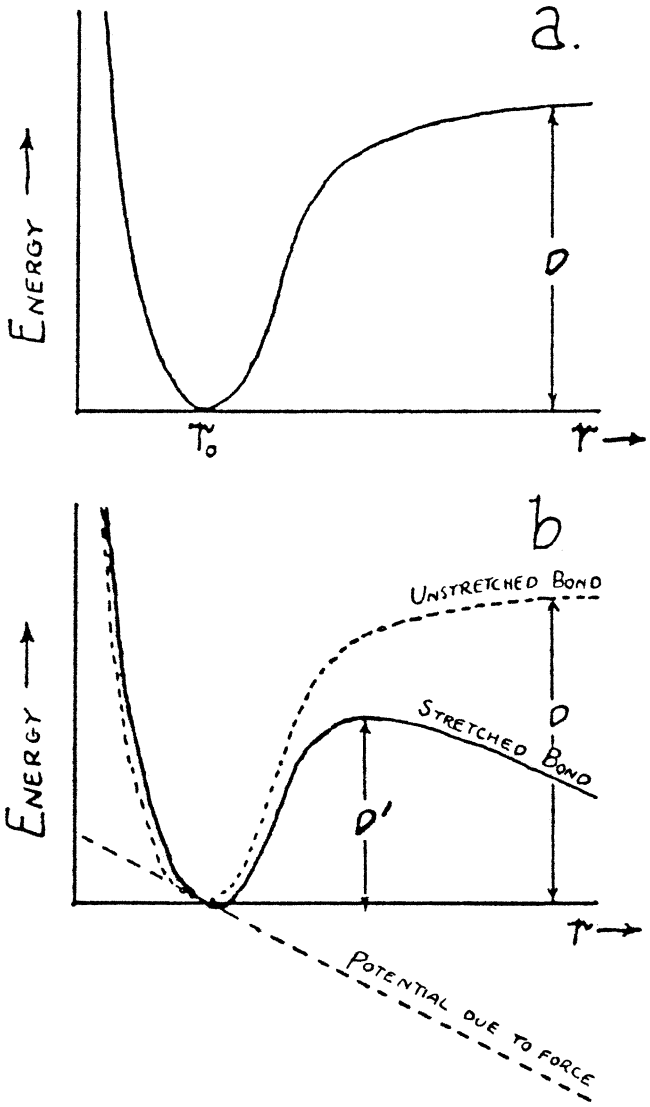

Figure 17. (a) Morse potential of a covalent bond, with equilibrium bond length r_0 and dissociation energy D. (b) Morse potential deformed by an external force F, resulting in a diminished barrier D' for dissociation. Reprinted with permission from ref 38. Copyright 1940, American Chemical Society, Washington, DC.

Table 7. Room Temperature Rupture Forces F_{rup} (nN) of Selected Covalent Bonds as a Function of Lifetime τ[a]

		⟨F⟩ (nN)				
bond	model molecule	τ = 1 ps	τ = 1 μs	τ = 1 s	τ = 10^6 s	τ = 10^{12} s
C−C	$H_3CCH_2CH_3$	6.1	4.7	3.8	3.1	2.5
C−N	H_3CNHCH_3	6.3	4.8	3.8	3.0	2.3
C−O	H_3COCH_3	6.6	5.0	4.0	3.2	2.5
Si−C	$H_3SiCH_2CH_3$	4.3	3.3	2.6	2.1	1.6
Si−N	$H_3SiNHCH_3$	4.3	3.3	2.7	2.2	1.7
Si−O	H_3SiOCH_3	4.8	3.8	3.1	2.6	2.2
Si−Si	$H_3SiSiH_2SiH_3$	3.0	2.2	1.7	1.3	0.9

[a] Data taken from ref 323.

tively high forces of ≥1 nN. Interestingly, over the different lifetime regimes, the relative mechanical bond strength is not conserved: at ultrashort time scales, the C−N bond is more stable than the C−C bond, while at τ = 1 s, both are equally stable and the C−C bond exhibits a better long-term stability than the C−N bond.

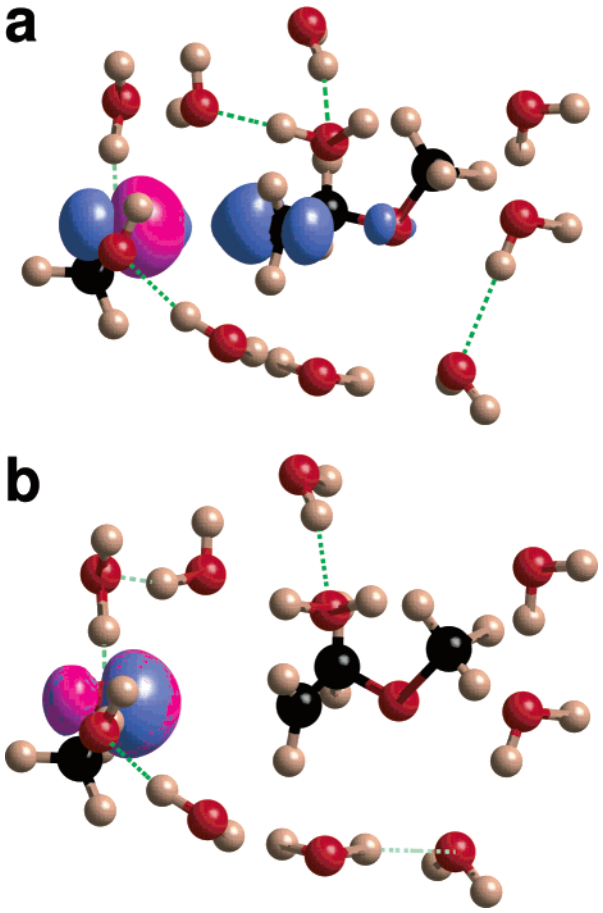

Figure 18. Orbitals of the breaking bond before and after the electron transfer. The two orbitals are plotted in blue and magenta, respectively, with like colors for positive and negative lobes. Before the electron transfer takes place, the two orbitals are clearly separated; after the electron transfer both orbitals occupy the same space. Reprinted with permission from ref 399. Copyright 2002, American Chemical Society, Washington, DC.

Röhrig and Frank used first-principles molecular dynamics simulations to study the behavior of *cis*-polyacetylene fragments under tensile stress.[324] They found that the barrier of a cis−trans isomerization of conjugated double bonds is lowered by the applied force but probably not sufficiently to induce the isomerization in an AFM experiment. These authors also determined rupture forces directly from the simulations, as well as from a kinetic model, which treats the polymer as a system of linearly coupled springs. Interestingly, they observe a decrease of rupture forces with increasing chain length, from 8.9 nN for hexatriene to 6.3 nN for pentadecaene.

Until then, only homolytic bond cleavage was considered in the experimental and theoretical single-molecule studies in mechanochemistry.[322−324,351] Aktah and Frank pointed out that, in solution, also heterolytic bond cleavage is feasible, resulting in bond hydrolysis.[399] In their elegant study, they used again first-principles molecular dynamics to stretch a piece of poly(ethylene glycol) in a cluster of 10 water molecules. Hydrolysis is induced by formation of an ion pair, which results from heterolytic cleavage of a C−O bond, as illustrated in Figure 18.

Trying to develop this intriguing observation into a general mechanochemical concept, it was suggested

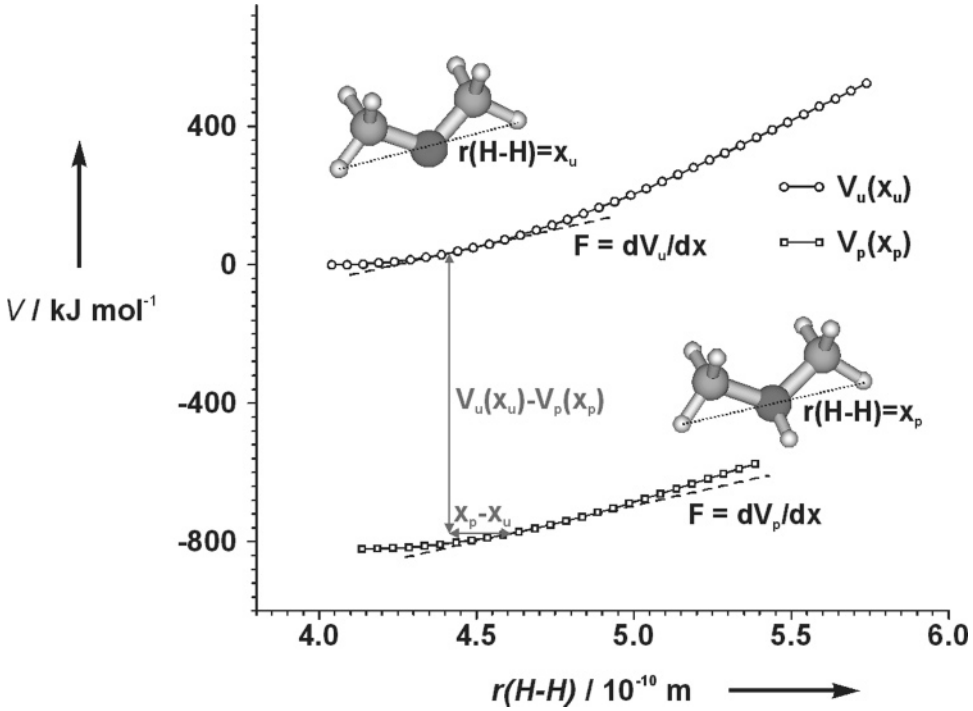

Figure 19. COGEF potentials for dimethyl ether (○) and protonated dimethyl ether (□). When an external force F is applied, the unprotonated and protonated molecules are elongated to distances $r(\mathrm{H-H}) = x_u$ and x_p, respectively. The proton affinity under force consists of the potential difference $V_p(x_p) - V_u(x_u)$ and the mechanical work performed by the force F over a distance $(x_p - x_u)$. Reprinted with permission from ref 234. Copyright 2003, Wiley-VCH.

to calculate the change of thermochemical quantities as a function of the external mechanical force.[234] In this work, the proton affinity of dimethyl ether was calculated as a function of external force. If two COGEF potential functions V_u and V_p of a molecule in its unprotonated and protonated form, respectively, are given, an external force F stretches the unprotonated molecule to a length x_u, which is defined by $dV_u(x_u)/dx = F$. As soon as a proton binds, the molecule takes on the new length x_p with $dV_p(x_p)/dx = F$. This defines the proton affinity as a function of an external mechanical force F:

$$\mathrm{PA}(F) = -[V_p(x_p) - V_u(x_u)] + (x_p - x_u)F \quad (8)$$

The first minus sign in eq 8 is necessary because potentials are negative, while proton affinity is defined as a positive value. Figure 19 illustrates the meaning of this equation, where dimethyl ether is chosen as a simple model system. PA(F) consists of a chemical contribution, the difference of the potential functions $(V_u - V_p)$, and a purely mechanical contribution, the force acting over the length increase $(x_p - x_u)$. This mechanical contribution is supplied by the environment, e.g., by the force exerted through an AFM cantilever.

It is, however, more instructive to calculate the force-induced change in proton affinity $\Delta\mathrm{PA}(F)$, which amounts to

$$\Delta\mathrm{PA}(F) = \mathrm{PA}(F) - \mathrm{PA}(0) \quad (9)$$

The result is displayed graphically in Figure 20. For small values of F, the function is almost linear. This regime is dominated by the contribution $(x_p - x_u)F$, which is a good approximation of the length difference between the protonated and unprotonated unstretched molecule $(x_{p,0} - x_{u,0})$ times the applied force. This illustrates the low-force limit, where the force-induced change in proton affinity is solely due to the different equilibrium geometries of the species in question.

4. Conclusions and Outlook

We have presented the crucial evidence accumulated over the last 100 years that mechanochemical activation actually exists. Polymers undergo main-chain scission in the center, which is the point where the maximum of viscous forces is reached. Viscous flow, as well as milling, drilling, or sawing, generates mechanoradicals, even at low temperatures. These radicals have been assigned via their ESR spectra. Overall, the picture is concise and conclusive. A local thermal activation of these processes can be ruled out, because the temperatures necessary for radical formation are simply too high and thermal activation would not selectively cleave the polymer backbone in the middle. Recent experimental and theoretical advances like atomic force microscopy and DFT-based molecular dynamics simulations allow the investigation of the bond cleavage process at the single-molecule level. Bond-rupture forces in the range of a few nanonewtons are commonly measured for various types of covalent bonds. The experimental values are in reasonable agreement with the calculations.

In addition, the theory allows for watching the molecule dissociate and to identify reaction pathways other than homolytic bond cleavage. Mechanically induced bond hydrolysis was suggested based on the results from experimental studies of bulk polymers. The detailed mechanism is revealed in quantum

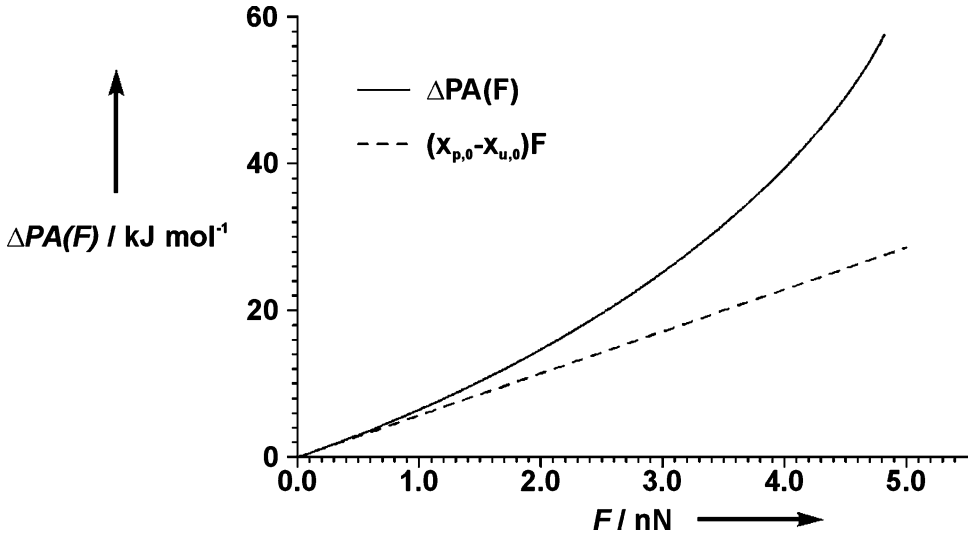

Figure 20. Force-induced change in proton affinity $\Delta PA(F)$ of dimethyl ether. For small forces, the mechanical work $(x_{p,0} - x_{u,0})F$ is an excellent approximation, which is illustrated by the dashed line. For higher forces, the softening of the bonds upon protonation becomes important. The same force stretches the protonated molecule more than the unprotonated one. When both effects act together, the softening of the bond and the lengthening of the molecule upon protonation lead to a drastic increase in proton affinity of up to 60 kJ/mol under the influence of an external force. Reprinted with permission from ref 234. Copyright 2003, Wiley-VCH.

molecular dynamics simulations. Also the mechanochemical formation of metal nanowires is understood in a close interaction of the experiment and theory. New concepts, like the calculation of thermochemical values as a function of the mechanical force, may provide an intuitive framework for these processes, which can aid both experimental and theoretical researchers in their work.

On the basis of the available experimental and theoretical results, one can identify the peculiar characteristics of mechanochemistry, which are quite intriguing. Because force is directional, mechanical bond activation is selective. High-energy processes such as homolytic bond cleavage, also called mechanolysis, occur even at low temperatures. Mechanically activated bond hydrolysis is selectively occurring in the presence of water. Because the fragments are rapidly separated, mechanochemically induced bond cleavage is often also irreversible. Technological applications of mechanochemistry are older than the systematic investigation of the underlying processes. Especially the potential for "green" chemistry is currently explored. In solid-state chemistry, mechanochemistry is a well-established branch, which holds regular international conferences.

With increasing knowledge of the underlying molecular processes, more phenomena may be identified as being truly mechanochemical. Thus far, the conceptual understanding has become more refined. While the early picture of mechanical activation largely was that mechanical energy was somehow accumulated in the activated bond, it is now clear that the mechanical energy resides mostly in the environment, which acts as a reservoir of mechanical energy, like a spring under tension. Not all of the energy necessary for bond rupture has to go into the bond. The transition state is reached much earlier, and the environment funnels the proper amount of energy into the bond by pulling the molecule apart, while the environment relaxes.

Mechanical activation of chemical bonds is present in a large number of everyday processes. We hope that the basic ideas of mechanochemistry are soon taught in undergraduate level physical or general chemistry classes. Addition of a mechanical potential to a potential-energy surface, as shown in Figure 17, is conceptually and formally similar to the addition of an electric potential in electrochemistry and provides the necessary insight. We hope that terms such as mechanochemistry, mechanoradical, mechanolysis, and mechanical activation are soon to be found in the index of textbooks in general, physical, and polymer chemistry.

5. Acknowledgments

The authors thank Hermann E. Gaub, Michel Grandbois, and Matthias Rief for helpful discussions. Vladimír Šepelák provided reprints of his work. Nicolas Agraït, Peter Baláž, Ragnar Erlandsson, Irmgard Frank, and David Tyler provided electronic versions of previously published figures. Valuable comments on the manuscript were received from Tuan Q. Nguyen. Financial support from the Fonds der Chemischen Industrie (to M. K. B.) is gratefully acknowledged.

6. References

(1) Boldyrev, V. V.; Tkácová, K. *J. Mater. Synth. Proc.* **2000**, *8*, 121.
(2) Baláž, P. *Int. J. Miner. Process.* **2003**, *72*, 341.
(3) Takacs, L. *J. Minerals Met. Mater. Soc.* **2000**, *52*, 12.
(4) Ostwald, W. *Lehrbuch der Allgemeinen Chemie, Board 1 Stöchiometrie*; Engelmann: Leipzig, Germany, 1885.
(5) Ostwald, W. *Lehrbuch der Allgemeinen Chemie, Board 2.1 Verwandtschaftslehre*, 2nd ed.; Engelmann: Leipzig, Germany, 1896−1902.
(6) Ostwald, W. *Lehrbuch der Allgemeinen Chemie, Board 2.1 Chemische Energie*, 2nd ed.; 3rd Print; Engelmann: Leipzig, Germany, 1911.
(7) *Handbuch der Allgemeinen Chemie. Band 1: Die chemische Literatur und die Organisation der Wissenschaft*; Ostwald, W., Drucker, C., Eds.; Akademische Verlagsgesellschaft m. b. H.: Leipzig, Germany, 1919; p 77.

(8) Gilman, J. J. *Science* **1996**, *274*, 65.
(9) Website of the Institute of Solid State Chemistry and Mechanochemistry; http://www.solid.nsc.ru/.
(10) Tkácová, K. *J. Mater. Synth. Proc.* **2000**, *8*, 119.
(11) Krüger, D.; Rousseau, R.; Fuchs, H.; Marx, D. *Angew. Chem. Int. Ed.* **2003**, *42*, 2251.
(12) Heegn, H. *Chem. Ing. Technol.* **2001**, *73*, 1529.
(13) Mendoza, J. P. M.; Valenzuela, O. E. A.; Flores, V. C.; Aquino, J. M.; De la Torre, S. D. *J. Alloys Compd.* **2004**, *369*, 144.
(14) Rief, M.; Grubmuller, H. *ChemPhysChem* **2002**, *3*, 255.
(15) Zhuang, X. W.; Rief, M. *Curr. Opin. Struct. Biol.* **2003**, *13*, 88.
(16) Carrion-Vazquez, M.; Oberhauser, A. F.; Fisher, T. E.; Marszalek, P. E.; Li, H.; Fernandez, J. M. *Prog. Biophys. Mol. Biol.* **2000**, *74*, 63.
(17) Merkel, R. *Phys. Rep.* **2001**, *346*, 344.
(18) Thompson, L. H.; Doraiswamy, L. K. *Ind. Eng. Chem. Res.* **1999**, *38*, 1215.
(19) Luche, J. L. *Ultrason.* **1992**, *30*, 156.
(20) Boldyrev, V. V. *Ultrason. Sonochem.* **1995**, *2*, S143.
(21) Nguyen, T. Q.; Liang, Q. Z.; Kausch, H. H. *Polymer* **1997**, *38*, 3783.
(22) Cohn, S. A. *Mol. Chem. Neuropathol.* **1990**, *12*, 83.
(23) Cross, R. A. *Nature* **1997**, *385*, 18.
(24) Visscher, K.; Schnitzer, M. J.; Block, S. M. *Nature* **1999**, *400*, 184.
(25) Schnitzer, M. J.; Visscher, K.; Block, S. M. *Nat. Cell Biol.* **2000**, *2*, 718.
(26) Bustamante, C.; Keller, D.; Oster, G. *Acc. Chem. Res.* **2001**, *34*, 412.
(27) Howard, J. *Mechanics of Motor Proteins and the Cytoskeleton*; Sinauer Associates, Inc.: Sunderland, U.K., 2001.
(28) Robinson, D. N.; Girard, K. D.; Octtaviani, E.; Reichl, E. M. *J. Muscle Res. Cell Motility* **2002**, *23*, 719.
(29) Katchalsky, A.; Zwick, M. *J. Polymer Sci.* **1955**, *16*, 221.
(30) Urry, D. W. *J. Phys. Chem. B* **1997**, *101*, 11007.
(31) Urry, D. W. *J. Protein Chem.* **1988**, *7*, 1.
(32) Berezin, I. V.; Klibanov, A. M.; Martinek, K. *Biochim. Biophys. Acta* **1974**, *364*, 193.
(33) Klibanov, A. M.; Samokhin, G. P.; Martinek, K.; Berezin, I. V. *Biochim. Biophys. Acta* **1976**, *438*, 1.
(34) Staudinger, H.; Leupold, E. O. *Ber. Deutsch. Chem. Ges.* **1930**, *63*, 730.
(35) Staudinger, H.; Bondy, H. F. *Ber. Deutsch. Chem. Ges.* **1930**, *63*, 734.
(36) Staudinger, H. *Ber. Deutsch. Chem. Ges.* **1930**, *63*, 921.
(37) Staudinger, H.; Heuer, W. *Ber. Deutsch. Chem. Ges.* **1934**, *67*, 1159.
(38) Kauzmann, W.; Eyring, H. *J. Am. Chem. Soc.* **1940**, *62*, 3113.
(39) Frenkel, J. *Acta Physicochim. U.R.S.S.* **1944**, *19*, 51.
(40) Nguyen, T. Q.; Kausch, H. H. *Macromolecules* **1990**, *23*, 5137.
(41) Nguyen, T. Q. *Chimia* **2001**, *55*, 147.
(42) Buchholz, B. A.; Zahn, J. M.; Kenward, M.; Slater, G. W.; Barron, A. E. *Polymer* **2004**, *45*, 1223.
(43) Kuijpers, M. W. A.; Iedema, P. D.; Kemmere, M. F.; Keurentjes, J. T. F. *Polymer* **2004**, *45*, 6461.
(44) Sivalingam, G.; Agarwal, N.; Madras, G. *AIChE J.* **2004**, *50*, 2258.
(45) Jellinek, H. H. G. *Degradation of Vinyl Polymers*; Academic Press: New York, 1955.
(46) Porter, R. S.; Johnson, J. F. *J. Phys. Chem.* **1959**, *63*, 202.
(47) Nguyen, T. Q.; Kausch, H. H. *Adv. Polym. Sci.* **1992**, *100*, 73.
(48) Because of the historic circumstances, the results seem to have been overgeneralized in the literature. The paper appeared in a Soviet journal in 1944, in an issue that because of the war times was not as widely circulated as usual. It is very difficult to find in libraries. The text is available in English.
(49) Rehner, J., Jr. *J. Chem. Phys.* **1945**, *13*, 450.
(50) Harrington, R. E.; Zimm, B. H. *J. Phys. Chem.* **1965**, *69*, 161.
(51) Odell, J. A.; Keller, A.; Miles, M. J. *Polym. Commun.* **1983**, *24*, 7.
(52) Odell, J. A.; Keller, A. *J. Polym. Sci. B* **1986**, *24*, 1889.
(53) Odell, J. A.; Keller, A.; Rabin, Y. *J. Chem. Phys.* **1988**, *88*, 4022.
(54) Odell, J. A.; Muller, A. J.; Narh, K. A.; Keller, A. *Macromolecules* **1990**, *23*, 3092.
(55) Nguyen, T. Q.; Kausch, H. H. *Polymer* **1992**, *33*, 2611.
(56) Muller, A. J.; Odell, J. A.; Carrington, S. *Polymer* **1992**, *33*, 2598.
(57) Odell, J. A.; Keller, A.; Muller, A. J. *Colloid Polym. Sci.* **1992**, *270*, 307.
(58) Merrill, E. W.; Horn, A. F. *Polym. Commun.* **1984**, *25*, 144.
(59) Nguyen, T. Q.; Kausch, H. H. *Chimia* **1986**, *40*, 129.
(60) Zhurkov, S. N.; Korsukov, V. E. *J. Polym. Sci. B* **1974**, *12*, 385.
(61) Nguyen, T. Q.; Kausch, H. H. *Colloid Polym. Sci.* **1986**, *264*, 764.
(62) Casale, A. *J. Appl. Polym. Sci.* **1975**, *19*, 1461.
(63) *Flexible Polymer Chains in Elongational Flow. Theory and Experiment*; Nguyen, T. Q., Kausch, H. H., Eds.; Springer-Verlag: Berlin, Germany, 1999.
(64) Doerr, T. P.; Taylor, P. L. *J. Chem. Phys.* **1994**, *101*, 10107.
(65) Cascales, J. J. L.; Martinez, M. C. L. *An. Quim.* **1991**, *87*, 655.
(66) Cascales, J. J. L.; Delatorre, J. G. *J. Chem. Phys.* **1991**, *95*, 9384.
(67) Cascales, J. J. L.; Delatorre, J. G. *J. Chem. Phys.* **1992**, *97*, 4549.
(68) Oliveira, F. A.; Taylor, P. L. *J. Chem. Phys.* **1994**, *101*, 10118.
(69) Oliveira, F. A. *Phys. Rev. B* **1998**, *57*, 10576.
(70) Puthur, R.; Sebastian, K. L. *Phys. Rev. B* **2002**, *66*, 024304.
(71) Maroja, A. M.; Oliveira, F. A.; Ciesla, M.; Longa, L. *Phys. Rev. E* **2001**, *63*, 061801.
(72) Toda, F. *Synlett* **1993**, 303.
(73) Toda, F. *Acc. Chem. Res.* **1995**, *28*, 480.
(74) Watson, W. F. *Makromol. Chem.* **1959**, *34*, 240.
(75) Sohma, J. *Prog. Polym. Sci.* **1989**, *14*, 451.
(76) Pike, M.; Watson, W. F. *J. Polymer Sci.* **1952**, *9*, 229.
(77) Ayrey, G.; Moore, C. G.; Watson, W. F. *J. Polymer Sci.* **1956**, *19*, 1.
(78) Zhurkov, S. N.; Narzullaev, B. N. *Zh. Tekh. Fiz.* **1953**, *23*, 1677.
(79) Zhurkov, S. N. *Intern. J. Fracture Mech.* **1965**, *1*, 311.
(80) Zhurkov, S. N.; Tomashevskii, E. E.; Savostin, A. Y. *Dokl. Akad. Nauk S.S.S.R.* **1964**, *159*, 303.
(81) Zhurkov, S. N.; Zakrevskii, V. A.; Tomashevskii, E. E. *Sov. Phys. Solid State* **1964**, *6*, 1508.
(82) Backman, D. K.; Devries, K. L. *J. Polym. Sci. A-1* **1969**, *7*, 2125.
(83) Devries, K. L.; Roylance, D. K.; Williams, M. L. *J. Polym. Sci. A-1* **1970**, *8*, 237.
(84) Campbell, D.; Peterlin, A. *J. Polym. Sci. B* **1968**, *6*, 481.
(85) Becht, J.; Fischer, H. *Kolloid-Z. Z. Polym.* **1970**, *240*, 766.
(86) Verma, G. S. P.; Peterlin, A. *Kolloid-Z. Z. Polym.* **1970**, *236*, 111.
(87) Becht, J.; Fischer, H. *Kolloid-Z. Z. Polym.* **1969**, *229*, 167.
(88) Kausch-Blecken von Schmeling, H. H. *J. Macromol. Sci.-Rev. Macromol. Chem.* **1970**, *C 4*, 243.
(89) Kolbert, A. C.; Didier, J. G.; Xu, L. S. *Macromolecules* **1996**, *29*, 8591.
(90) Zhurkov, S. N.; Novak, I. I.; Vettegren, V. I. *Dokl. Akad. Nauk S.S.S.R.* **1964**, *157*, 1431.
(91) Zhurkov, S. N.; Vettegren, V. I.; Novak, I. I.; Kashints, Kn. *Dokl. Akad. Nauk S.S.S.R.* **1967**, *176*, 623.
(92) Zhurkov, S. N.; Vettegren, V. I.; Korsukov, V. E.; Novak, I. I. *Sov. Phys. Solid State* **1969**, *11*, 233.
(93) Roylance, D. K.; Devries, K. L. *J. Polym. Sci. B* **1971**, *9*, 443.
(94) Vettegren, V. I.; Novak, I. I. *J. Polym. Sci. B* **1973**, *11*, 2135.
(95) Vettegren, V. I.; Novak, I. I.; Friedland, K. J. *Int. J. Fracture* **1975**, *11*, 789.
(96) Sakaguchi, M.; Yamakawa, H.; Sohma, J. *J. Polym. Sci. C* **1974**, *12*, 193.
(97) Sakaguchi, M.; Sohma, J. *J. Polym. Sci. B* **1975**, *13*, 1233.
(98) Nagamura, T.; Takayanagi, M. *J. Polym. Sci. B* **1975**, *13*, 567.
(99) Nagamura, T.; DeVries, K. L. *Polym. Eng. Sci.* **1979**, *19*, 89.
(100) Brown, I. M.; Sandreczki, T. C. *Macromolecules* **1985**, *18*, 1041.
(101) Kaptan, H. Y.; Tatar, L. *J. Appl. Polym. Sci.* **1997**, *65*, 1161.
(102) Tatar, L.; Kaptan, H. Y. *J. Polym. Sci. B* **1997**, *35*, 2195.
(103) Kuzuya, M.; Yamauchi, Y.; Kondo, S. *J. Phys. Chem. B* **1999**, *103*, 8051.
(104) Kondo, S. I.; Sasai, Y.; Hosaka, S.; Ishikawa, T.; Kuzuya, M. *J. Polym. Sci. A* **2004**, *42*, 4161.
(105) Sasai, Y.; Yamauchi, Y.; Kondo, S.; Kuzuya, M. *Chem. Pharm. Bull.* **2004**, *52*, 339.
(106) Kuzuya, M.; Kondo, S. I.; Noguchi, A.; Noda, N. *J. Polym. Sci. B* **1992**, *30*, 97.
(107) Popov, A. A.; Zaikov, G. E. *J. Macromol. Sci.-Rev. Macromol. Chem. Phys.* **1987**, *C27*, 379.
(108) Bershtein, V. A.; Egorova, L. M. *Vysokomol. Soedin. Ser. A* **1977**, *19*, 1260.
(109) Krasheninnikova, G. A.; Popov, A. A.; Kaganskii, M. M.; Privalova, L. G.; Zaikov, G. Y. *Vysokomol. Soedin. Ser. A* **1985**, *27*, 2391.
(110) Popov, A. A.; Krisyuk, B. E.; Blinov, N. N.; Zaikov, G. E. *Eur. Polym. J.* **1981**, *17*, 169.
(111) Popov, A. A.; Blinov, N. N.; Krisyuk, B. E.; Karpova, S. G.; Neverov, A. N.; Zaikov, G. Y. *Vysokomol. Soedin. Ser. A* **1981**, *23*, 1510.
(112) Popov, A. A.; Krisyuk, B. E.; Zaikov, G. Y. *Vysokomol. Soedin. Ser. A* **1980**, *22*, 1366.
(113) Popov, A. A.; Blinov, N. N.; Krisyuk, B. E.; Zaikov, G. E. *Eur. Polym. J.* **1982**, *18*, 413.
(114) Popov, A. A.; Blinov, N. N.; Krisyuk, B. E.; Karpova, S. G.; Privalova, L. G.; Zaikov, G. E. *J. Polym. Sci. B* **1983**, *21*, 1017.
(115) Popov, A. A.; Krisiuk, B. E.; Blinov, N. N.; Zaikov, G. E. *Dokl. Akad. Nauk S.S.S.R.* **1980**, *253*, 1169.
(116) Krisyuk, B. E.; Popov, A. A.; Zaikov, G. Y. *Vysokomol. Soedin. Ser. A* **1980**, *22*, 329.
(117) Rapoport, N. Y.; Livanova, N. M.; Grigorev, A. G.; Zaikov, G. Y. *Vysokomol. Soedin. Ser. A* **1983**, *25*, 2188.
(118) Rapoport, N. Y.; Zaikov, G. E. *Usp. Khim.* **1983**, *52*, 1568.
(119) Popov, A. A.; Zaikov, G. E. *Int. J. Polym. Mater.* **1992**, *17*, 143.
(120) Tabata, M.; Yamakawa, H.; Takahashi, K.; Sohma, J. *Polym. Degrad. Stab.* **1979**, *1*, 57.
(121) Dimier, F.; Vergnes, B.; Vincent, M. *Rheol. Acta* **2004**, *43*, 196.
(122) Bartels, H.; Scholz, G. *Kautsch. Gummi Kunstst.* **1993**, *46*, 361.
(123) Angier, D. J.; Chambers, W. T.; Watson, W. F. *J. Polymer Sci.* **1957**, *25*, 129.

(124) Kreft, R.; Ernst, K.; Marinow, S. *Kautsch. Gummi Kunstst.* **1996**, *49*, 504.
(125) Leblanc, J. L.; Lionnet, R. *Polym. Eng. Sci.* **1992**, *32*, 989.
(126) Scholz, B. *Kautsch. Gummi Kunstst.* **1980**, *33*, 716.
(127) Harmon, D. J.; Jacobs, H. L. *J. Appl. Polym. Sci.* **1966**, *10*, 253.
(128) Frendel, A.; Drache, M.; Janke, G.; Schmidt-Naake, G. *Chem. Ing. Technol.* **2000**, *72*, 391.
(129) Schmidt-Naake, G.; Frendel, A.; Drache, M.; Janke, G. *Chem. Eng. Technol.* **2001**, *24*, 889.
(130) Smith, A. P.; Shay, J. S.; Spontak, R. J.; Balik, C. M.; Ade, H.; Smith, S. D.; Koch, C. C. *Polymer* **2000**, *41*, 6271.
(131) White, J. L.; Sasaki, A. *Polym. Plast. Techn. Engin.* **2003**, *42*, 711.
(132) Janke, G.; Schmidt-Naake, G. *Chem. Ing. Technol.* **2001**, *73*, 99.
(133) Janke, G.; Frendel, A.; Schmidt-Naake, G. *Chem. Eng. Technol.* **1999**, *22*, 997.
(134) Janke, G.; Frendel, A.; Schmidt-Naake, G. *Chem. Ing. Technol.* **1999**, *71*, 496.
(135) Janke, G.; Schmidt-Naake, G. *Chem. Eng. Technol.* **2001**, *24*, 711.
(136) Hasegawa, M.; Akiho, Y.; Kanda, Y. *J. Appl. Polym. Sci.* **1995**, *55*, 297.
(137) Hasegawa, M.; Honma, T.; Ishiyama, S.; Kanda, Y. *Kagaku Kogaku Ronbunshu* **1991**, *17*, 1019.
(138) Hasegawa, M.; Kimata, M.; Kobayashi, S. I. *J. Appl. Polym. Sci.* **2001**, *82*, 2849.
(139) Hasegawa, M.; Kimata, M.; Kobayashi, S. I. *J. Appl. Polym. Sci.* **2002**, *84*, 2011.
(140) Schmidt-Naake, G.; Drache, M.; Weber, M. *Macromol. Chem. Phys.* **2002**, *203*, 2232.
(141) Liu, C. S.; Wang, Q. *J. Appl. Polym. Sci.* **2000**, *78*, 2191.
(142) Zhao, J. R.; Feng, Y.; Chen, X. F. *J. Appl. Polym. Sci.* **2004**, *91*, 282.
(143) Nesarikar, A. R.; Carr, S. H.; Khait, K.; Mirabella, F. M. *J. Appl. Polym. Sci.* **1997**, *63*, 1179.
(144) Khait, K.; Torkelson, J. M. *Polym. Plast. Techn. Engin.* **1999**, *38*, 445.
(145) Kuzuya, M.; Kondo, S. I.; Noguchi, A. *Macromolecules* **1991**, *24*, 4047.
(146) Kondo, S.; Hosaka, S.; Sasai, Y.; Kuzuya, M. *Chem. Pharm. Bull.* **2004**, *52*, 1302.
(147) Kondo, S.; Sasai, Y.; Kosaki, M.; Kuzuya, M. *Chem. Pharm. Bull.* **2004**, *52*, 488.
(148) Kondo, S.; Sasai, Y.; Kuzuya, M.; Furukawa, S. *Chem. Pharm. Bull.* **2002**, *50*, 1434.
(149) Kuzuya, M.; Sasai, Y.; Mouri, M.; Kondo, S. *Thin Solid Films* **2002**, *407*, 144.
(150) Kondo, S.; Hatakeyama, I.; Hosaka, S.; Kuzuya, M. *Chem. Pharm. Bull.* **2000**, *48*, 1882.
(151) Graiver, D.; Waikul, L. H.; Berger, C.; Narayan, R. *J. Appl. Polym. Sci.* **2004**, *92*, 3231.
(152) Birke, V.; Mattik, J.; Runne, D. *J. Mater. Sci.* **2004**, *39*, 5111.
(153) Hall, A. K.; Harrowfield, J. M.; Hart, R. J.; McCormick, P. G. *Environ. Sci. Technol.* **1996**, *30*, 3401.
(154) Boyde, S. *Green Chem.* **2002**, *4*, 293.
(155) Kajdas, C.; Bhushan, B. *J. Inf. Stor. Proc. Syst.* **1999**, *1*, 303.
(156) Klein, J. *Annu. Rev. Mater. Sci.* **1996**, *26*, 581.
(157) Bhushan, B.; Israelachvili, J. N.; Landman, U. *Nature* **1995**, *374*, 607.
(158) Israelachvili, J. N.; Tabor, D. *Proc. R. Soc. London, Ser. A* **1972**, *331*, 19.
(159) Singer, I. L. *J. Vac. Sci. Technol. A* **1994**, *12*, 2605.
(160) Tamai, Y. *J. Jpn. Soc. Lubr. Eng.* **1983**, *28*, 231.
(161) Shenghua, L.; He, Y.; Yuansheng, J. *Int. J. Mol. Sci.* **2004**, *5*, 13.
(162) Aharoni, S. M. *J. Appl. Polym. Sci.* **1972**, *16*, 3275.
(163) Vettegren, V. I.; Tshmel, A. E. *Eur. Polym. J.* **1976**, *12*, 853.
(164) Ábbas, K. B.; Kirschner, T.; Porter, R. S. *Eur. Polym. J.* **1978**, *14*, 361.
(165) Turssi, C. P.; Purquerio, B. D. M.; Serra, M. C. *J. Biomed. Mater. Res. B* **2003**, *65*, 280.
(166) Batchelor, A. W.; Stachowiak, G. W. *J. Orthop. Rheumatol.* **1996**, *9*, 3.
(167) Batchelor, A. W.; Stachowiak, G. W. *J. Orthop. Rheumatol.* **1996**, *9*, 11.
(168) Muschiolik, G.; Rawel, H. M.; Hone, T. Z.; Heinzelmann, K. *Nahrung-Food* **1994**, *38*, 464.
(169) Dongowski, G.; Bock, W. *Nahrung-Food* **1989**, *33*, 37.
(170) Kroll, J.; Schweitzer, T.; Voigt, A. *Lebensmittelindustrie* **1987**, *34*, 11.
(171) Kroll, J.; Gassmann, B. *Nahrung-Food* **1986**, *30*, 93.
(172) Schaich, K. M.; Rebello, C. A. *Cereal Chem.* **1999**, *76*, 748.
(173) Onwulata, C. I.; Konstance, R. P.; Cooke, P. H.; Farrell, H. M. *J. Dairy Sci.* **2003**, *86*, 3775.
(174) van den Einde, R. M.; Akkermans, C.; van der Goot, A. J.; Boom, R. M. *Carbohydr. Polym.* **2004**, *56*, 415.
(175) van den Einde, R. M.; van der Goot, A. J.; Boom, R. M. *J. Food Sci.* **2003**, *68*, 2396.
(176) van den Einde, R. M.; Bolsius, A.; van Soest, J. J. G.; Janssen, L.; van der Goot, A. J.; Boom, R. M. *Carbohydr. Polym.* **2004**, *55*, 57.
(177) Butyagin, P. Y. *Usp. Khim.* **1994**, *63*, 1031.
(178) Butyagin, P. *J. Mater. Synth. Proc.* **2000**, *8*, 205.
(179) Boldyrev, V. V. *Solid State Ionics* **1993**, *63*−*65*, 537.
(180) Fenoglio, I.; Martra, G.; Prandi, L.; Tomatis, M.; Coluccia, S.; Fubini, B. *J. Mater. Synth. Proc.* **2000**, *8*, 145.
(181) Molchanov, V. V.; Buyanov, R. A. *Kinet. Catal.* **2001**, *42*, 366.
(182) Mitchenko, S. A.; Khomutov, E. V.; Kovalenko, V. V.; Popov, A. F.; Beletskaya, I. P. *Inorg. Chim. Acta* **2001**, *320*, 31.
(183) Ivanov, E.; Suryanarayana, C. *J. Mater. Synth. Proc.* **2000**, *8*, 235.
(184) Šepelák, V. *Ann. Chim. Sci. Mater.* **2002**, *27*, 61.
(185) Šepelák, V.; Menzel, M.; Becker, K. D.; Krumeich, F. *J. Phys. Chem. B* **2002**, *106*, 6672.
(186) Šepelák, V.; Menzel, M.; Bergmann, I.; Wiebcke, M.; Krumeich, F.; Becker, K. D. *J. Magn. Magn. Mater.* **2004**, *272*−*276*, 1616.
(187) Šepelák, V.; Baabe, D.; Mienert, D.; Litterst, F. J.; Becker, K. D. *Scr. Mater.* **2003**, *48*, 961.
(188) Šepelák, V.; Baabe, D.; Mienert, D.; Schultze, D.; Krumeich, F.; Litterst, F. J.; Becker, K. D. *J. Magn. Magn. Mater.* **2003**, *257*, 377.
(189) Šepelák, V.; Schultze, D.; Krumeich, F.; Steinike, U.; Becker, K. D. *Solid State Ionics* **2001**, *141*, 677.
(190) Druska, P.; Steinike, U.; Šepelák, V. *J. Solid State Chem.* **1999**, *146*, 13.
(191) Šepelák, V.; Steinike, U.; Uecker, D. C.; Wissmann, S.; Becker, K. D. *J. Solid State Chem.* **1998**, *135*, 52.
(192) Schüth, F.; Bogdanovic, B.; Felderhoff, M. *Chem. Commun.* **2004**, 2249.
(193) Jensen, C. M.; Zidan, R.; Mariels, N.; Hee, A.; Hagen, C. *Int. J. Hydrogen Energy* **1999**, *24*, 461.
(194) Zidan, R. A.; Takara, S.; Hee, A. G.; Jensen, C. M. *J. Alloys Compd.* **1999**, *285*, 119.
(195) Felderhoff, M.; Klementiev, K.; Grunert, W.; Spliethoff, B.; Tesche, B.; von Colbe, J. M. B.; Bogdanovic, B.; Hartel, M.; Pommerin, A.; Schüth, F.; Weidenthaler, C. *Phys. Chem. Chem. Phys.* **2004**, *6*, 4369.
(196) Meisner, G. P.; Tibbetts, G. G.; Pinkerton, F. E.; Olk, C. H.; Balogh, M. P. *J. Alloys Compd.* **2002**, *337*, 254.
(197) von Colbe de Bellosta, J.; Bogdanovic, B.; Felderhoff, M.; Pommerin, A.; Schüth, F. *J. Alloys Compd.* **2004**, *370*, 104.
(198) Dymova, T. N.; Mal'tseva, N. N.; Konoplev, V. N.; Golovanova, A. I.; Aleksandrov, D. P.; Sizareva, A. S. *Russ. J. Coord. Chem.* **2003**, *29*, 385.
(199) Mal'tseva, N. N.; Golovanova, A. I.; Dymova, T. N.; Aleksandrov, D. P. *Russ. J. Inorg. Chem.* **2001**, *46*, 1793.
(200) Dymova, T. N.; Konoplev, V. N.; Sizareva, A. S.; Aleksandrov, D. P. *Russ. J. Coord. Chem.* **2000**, *26*, 531.
(201) Zaluska, A.; Zaluski, L.; Ström-Olsen, J. O. *J. Alloys Compd.* **2000**, *307*, 157.
(202) Mulas, G.; Scudino, S.; Cocco, G. *Mater. Sci. Eng., A* **2004**, *375*−*377*, 961.
(203) Balema, V. P.; Pecharsky, V. K.; Dennis, K. W. *J. Alloys Compd.* **2000**, *313*, 69.
(204) Kameda, J.; Saruwatari, K.; Tanaka, H. *J. Colloid Interface Sci.* **2004**, *275*, 225.
(205) Streletskii, A. N.; Morozova, O. S.; Berestetskaya, I. V.; Borunova, A. B.; Butyagin, P. J. Mechanochemical reactions in gas (H_2,Co) solid (Zr,a-NiZr) systems. In *Metastable, Mechanically Alloyed, and Nanocrystalline Materials*; 1996; Vol. 225, parts 1 and 2, p 539.
(206) Streletskii, A. N.; Morozova, O. S.; Berestetskaya, I. V.; Borunova, A. B. Hydrogenation of CO and C during mechanical treatment of Zr and Ni containing systems. In *Mechanically Alloyed, Metastable, and Nanocrystalline Materials*; 1998; Vol. 269−272, part 1, p 283.
(207) Field, L. D.; Sternhell, S.; Wilton, H. V. *Tetrahedron* **1997**, *53*, 4051.
(208) Martinelli, G.; Plescia, P. *Phys. Earth Planet. Inter.* **2004**, *142*, 205.
(209) Nikolaev, A. V.; Voitov, G. I.; Ammosov, S. M. *Dokl. Akad. Nauk S.S.S.R.* **1994**, *337*, 393.
(210) Braga, D.; Grepioni, F. *Angew. Chem., Int. Ed.* **2004**, *43*, 4002.
(211) Braga, D.; Maini, L.; Polito, M.; Mirolo, L.; Grepioni, F. *Chem. Eur. J.* **2003**, *9*, 4362.
(212) Kolotilov, S. V.; Addison, A. W.; Trofimenko, S.; Dougherty, W.; Pavlishchuk, V. V. *Inorg. Chem. Commun.* **2004**, *7*, 485.
(213) Braun, T.; Buvaribarcza, A.; Barcza, L.; Konkolythege, I.; Fodor, M.; Migali, B. *Solid State Ionics* **1994**, *74*, 47.
(214) Braun, T. *Fullerene Sci. Technol.* **1997**, *5*, 1291.
(215) Komatsu, K.; Wang, G. W.; Murata, Y.; Tanaka, T.; Fujiwara, K.; Yamamoto, K.; Saunders, M. *J. Org. Chem.* **1998**, *63*, 9358.
(216) Wang, G. W.; Komatsu, K.; Murata, Y.; Shiro, M. *Nature* **1997**, *387*, 583.
(217) Murata, Y.; Kato, N.; Fujiwara, K.; Komatsu, K. *J. Org. Chem.* **1999**, *64*, 3483.

(218) Peng, R. F.; Wang, G. W.; Shen, Y. B.; Li, Y. J.; Zhang, T. H.; Liu, Y. C.; Murata, Y.; Komatsu, K. *Synth. Commun.* **2004**, *34*, 2117.
(219) Ikeda, A.; Hayashi, K.; Konishi, T.; Kikuchi, J. *Chem. Commun.* **2004**, 1334.
(220) Zhang, T. H.; Wang, G. W.; Lu, P.; Li, Y. J.; Peng, R. F.; Liu, Y. C.; Murata, Y.; Komatsu, K. *Org. Biomol. Chem.* **2004**, *2*, 1698.
(221) Zhang, Z.; Dong, Y. W.; Wang, G. W.; Komatsu, K. *Chem. Lett.* **2004**, *33*, 168.
(222) Murata, Y.; Han, A. H.; Komatsu, K. *Tetrahedron Lett.* **2003**, *44*, 8199.
(223) Wang, G. W.; Ting-Hu, Z. A.; Li, Y. J.; Lu, P.; Zhan, H.; Liu, Y. C.; Murata, Y.; Komatsu, K. *Tetrahedron Lett.* **2003**, *44*, 4407.
(224) Wang, G. W.; Zhang, T. H.; Hao, E. H.; Jiao, L. J.; Murata, Y.; Komatsu, K. *Tetrahedron* **2003**, *59*, 55.
(225) Fujiwara, K.; Komatsu, K. *Org. Lett.* **2002**, *4*, 1039.
(226) Murata, Y.; Kato, N.; Komatsu, K. *J. Org. Chem.* **2001**, *66*, 7235.
(227) Komatsu, K.; Fujiwara, K.; Murata, Y. *Chem. Lett.* **2000**, 1016.
(228) Tanaka, T.; Komatsu, K. *Synth. Commun.* **1999**, *29*, 4397.
(229) Komatsu, K.; Fujiwara, K.; Murata, Y.; Braun, T. *J. Chem. Soc., Perkin Trans. 1* **1999**, 2963.
(230) Komatsu, K.; Murata, Y.; Wang, G. W.; Tanaka, T.; Kato, N.; Fujiwara, K. *Fullerene Sci. Technol.* **1999**, *7*, 609.
(231) Kunitake, M.; Uemura, S.; Ito, O.; Fujiwara, K.; Murata, Y.; Komatsu, K. *Angew. Chem. Int. Ed.* **2002**, *41*, 969.
(232) Constabel, F.; Geckeler, K. E. *Tetrahedron Lett.* **2004**, *45*, 2071.
(233) Ausman, K. D.; Rohrs, H. W.; Yu, M. F.; Ruoff, R. S. *Nanotechnology* **1999**, *10*, 258.
(234) Beyer, M. K. *Angew. Chem. Int. Ed.* **2003**, *42*, 4913.
(235) Malik, S.; Rösner, H.; Hennrich, F.; Böttcher, A.; Kappes, M. M.; Beck, T.; Auhorn, M. *Phys. Chem. Chem. Phys.* **2004**, *6*, 3540.
(236) Yu, M. F.; Files, B. S.; Arepalli, S.; Ruoff, R. S. *Phys. Rev. Lett.* **2000**, *84*, 5552.
(237) Yu, M. F.; Lourie, O.; Dyer, M. J.; Moloni, K.; Kelly, T. F.; Ruoff, R. S. *Science* **2000**, *287*, 637.
(238) Turcaniova, L.; Balaz, P. *J. Mater. Synth. Proc.* **2000**, *8*, 365.
(239) Nüchter, M.; Ondruschka, B.; Trotzki, R. *J. Prakt. Chem.* **2000**, *342*, 720.
(240) Fernandez-Bertran, J.; Alvarez, J. C.; Reguera, E. *Solid State Ionics* **1998**, *106*, 129.
(241) Fernandez-Bertran, J.; Reguera, E. *Solid State Ionics* **1996**, *93*, 139.
(242) Reguera, E.; Fernandez-Bertran, J.; Paneque, A.; Yee-Madeira, H. *Spectrosc. Lett.* **2004**, *37*, 191.
(243) Sohma, J. *Colloid Polym. Sci.* **1992**, *270*, 1060.
(244) Chen, R.; Tyler, D. R. *Macromolecules* **2004**, *37*, 5430.
(245) Kelly, C. T.; White, J. R. *Polym. Degrad. Stab.* **1997**, *56*, 367.
(246) Kelly, C. T.; Tong, L.; White, J. R. *J. Mater. Sci.* **1997**, *32*, 851.
(247) Tong, L.; White, J. R. *Polym. Degrad. Stab.* **1996**, *53*, 381.
(248) Busfield, W. K.; Taba, P. *Polym. Degrad. Stab.* **1996**, *51*, 185.
(249) Odonnell, B.; White, J. R. *J. Mater. Sci.* **1994**, *29*, 3955.
(250) Baumhardtneto, R.; Depaoli, M. A. *Polym. Degrad. Stab.* **1993**, *40*, 53.
(251) Baumhardtneto, R.; Depaoli, M. A. *Polym. Degrad. Stab.* **1993**, *40*, 59.
(252) Schoolenberg, G. E.; Vink, P. *Polymer* **1991**, *32*, 432.
(253) Igarashi, M.; Devries, K. L. *Polymer* **1983**, *24*, 769.
(254) Huvet, A.; Philippe, J.; Verdu, J. *Eur. Polym. J.* **1978**, *14*, 709.
(255) Tyler, D. R. *Coord. Chem. Rev.* **2003**, *246*, 291.
(256) Matsui, H.; Arrivo, S. M.; Valentini, J. J.; Weber, J. N. *Macromolecules* **2000**, *33*, 5655.
(257) Nichols, M. E.; Gerlock, J. L.; Smith, C. A. *Polym. Degrad. Stab.* **1997**, *56*, 81.
(258) Igarashi, M.; Devries, K. L. *Polymer* **1983**, *24*, 1035.
(259) Tyler, D. R.; Chen, R. *Macromol. Symp.* **2004**, *209*, 231.
(260) Chen, R.; Yoon, M.; Smalley, A.; Johnson, D. C.; Tyler, D. R. *J. Am. Chem. Soc.* **2004**, *126*, 3054.
(261) Plotnikov, V. G. *Dokl. Akad. Nauk S.S.S.R.* **1988**, *301*, 376.
(262) Baimuratov, E.; Saidov, D. S.; Kalontarov, I. Y. *Polym. Degrad. Stab.* **1993**, *39*, 35.
(263) Benachour, D.; Rogers, C. E. *ACS Symp. Ser.* **1981**, *151*, 263.
(264) Todres, Z. V. *J. Chem. Res., Synop.* **2004**, 89.
(265) Pisarenko, L. M.; Nikulin, V. I.; Blagorazumov, M. P.; Neiland, O. Y.; Paulinsh, L. L. *Bull. Acad. Sci. U.S.S.R. Div. Chem. Sci.* **1990**, *39*, 1379.
(266) Tipikin, D. S. *Russ. J. Phys. Chem.* **2001**, *75*, 1720.
(267) Hugel, T.; Holland, N. B.; Cattani, A.; Moroder, L.; Seitz, M.; Gaub, H. E. *Science* **2002**, *296*, 1103.
(268) Athanassiou, A.; Kalyva, M.; Lakiotaki, K.; Georgiou, S.; Fotakis, C. *Adv. Mater.* **2005**, *17*, 988.
(269) Röhrig, U. F.; Troppmann, U.; Frank, I. *Chem. Phys.* **2003**, *289*, 381.
(270) Bensimon, D. *Structure* **1996**, *4*, 885.
(271) Israelachvili, J. N. *Intermolecular and Surface Forces*, 2nd ed.; Academic Press: San Diego, CA, 1992.
(272) Israelachvili, J.; Wennerstrom, H. *Nature* **1996**, *379*, 219.
(273) Urbakh, M.; Klafter, J.; Gourdon, D.; Israelachvili, J. *Nature* **2004**, *430*, 525.
(274) Leckband, D. *J. Adhes.* **2004**, *80*, 409.
(275) Rief, M.; Oesterhelt, F.; Heymann, B.; Gaub, H. E. *Science* **1997**, *275*, 1295.
(276) Brant, D. A. *Curr. Opin. Struct. Biol.* **1999**, *9*, 556.
(277) Abu-Lail, N. I.; Camesano, T. A. *J. Microsc.* **2003**, *212*, 217.
(278) Mehta, A. D.; Rief, M.; Spudich, J. A. *J. Biol. Chem.* **1999**, *274*, 14517.
(279) Mehta, A. D.; Rief, M.; Spudich, J. A.; Smith, D. A.; Simmons, R. M. *Science* **1999**, *283*, 1689.
(280) Bockelmann, U.; Essevaz-Roulet, B.; Heslot, F. *Phys. Rev. Lett.* **1997**, *79*, 4489.
(281) Williams, M. C.; Rouzina, I. *Curr. Opin. Struct. Biol.* **2002**, *12*, 330.
(282) Bockelmann, U. *Curr. Opin. Struct. Biol.* **2004**, *14*, 368.
(283) Hansma, H. G.; Kasuya, K.; Oroudjev, E. *Curr. Opin. Struct. Biol.* **2004**, *14*, 380.
(284) Harris, S. A. *Contemp. Phys.* **2004**, *45*, 11.
(285) Rief, M.; Gautel, M.; Oesterhelt, F.; Fernandez, J. M.; Gaub, H. E. *Science* **1997**, *276*, 1109.
(286) Fisher, T. E.; Carrion-Vazquez, M.; Oberhauser, A. F.; Li, H.; Marszalek, P. E.; Fernandez, J. M. *Neuron* **2000**, *27*, 435.
(287) Moy, V. T.; Florin, E. L.; Gaub, H. E. *Science* **1994**, *266*, 257.
(288) Florin, E. L.; Moy, V. T.; Gaub, H. E. *Science* **1994**, *264*, 415.
(289) Heinz, W. F.; Hoh, J. H. *Trends Biotechnol.* **1999**, *17*, 143.
(290) Fisher, T. E.; Marszalek, P. E.; Fernandez, J. M. *Nat. Struct. Biol.* **2000**, *7*, 719.
(291) Clausen-Schaumann, H.; Seitz, M.; Krautbauer, R.; Gaub, H. E. *Curr. Opin. Chem. Biol.* **2000**, *4*, 524.
(292) Zlatanova, J.; Lindsay, S. M.; Leuba, S. H. *Prog. Biophys. Mol. Biol.* **2000**, *74*, 37.
(293) Evans, E. *Annu. Rev. Biophys. Biomol. Struct.* **2001**, *30*, 105.
(294) Janshoff, A.; Neitzert, M.; Oberdorfer, Y.; Fuchs, H. *Angew. Chem. Int. Ed.* **2000**, *39*, 3213.
(295) Hugel, T.; Seitz, M. *Macromol. Rapid Commun.* **2001**, *22*, 989.
(296) Reich, Z.; Kapon, R.; Nevo, R.; Pilpel, Y.; Zmora, S.; Scolnik, Y. *Biotechnol. Adv.* **2001**, *19*, 451.
(297) Hinterdorfer, P.; Gruber, H. J.; Kienberger, F.; Kada, G.; Riener, C.; Borken, C.; Schindler, H. *Colloids Surf., B* **2002**, *23*, 115.
(298) Hinterdorfer, P. Molecular recognition studies using the atomic force microscope. In *Atomic Force Microscopy in Cell Biology*; 2002; Vol. 68, p 115.
(299) Fotiadis, D.; Scheuring, S.; Muller, S. A.; Engel, A.; Muller, D. J. *Micron* **2002**, *33*, 385.
(300) Bustamante, C.; Bryant, Z.; Smith, S. B. *Nature* **2003**, *421*, 423.
(301) Zhang, W.; Zhang, X. *Prog. Polym. Sci.* **2003**, *28*, 1271.
(302) Allemand, J. F.; Bensimon, D.; Croquette, V. *Curr. Opin. Struct. Biol.* **2003**, *13*, 266.
(303) Smith, S. B.; Cui, Y. J.; Bustamante, C. Optical-trap force transducer that operates by direct measurement of light momentum. In *Biophotonics*; 2003; Vol. 361, part B, p 134.
(304) Dufrene, Y. F. *Curr. Opin. Microbiol.* **2003**, *6*, 317.
(305) Allen, S.; Rigby-Singleton, S. M.; Harris, H.; Davies, M. C.; O'Shea, P. *Biochem. Soc. Trans.* **2003**, *31*, 1052.
(306) Samori, P. *J. Mater. Chem.* **2004**, *14*, 1353.
(307) Santos, N. C.; Castanho, M. *Biophys. Chem.* **2004**, *107*, 133.
(308) Edwardson, J. M.; Henderson, R. M. *Drug Discovery Today* **2004**, *9*, 64.
(309) da Silva, L. P. *Protein Pept. Lett.* **2002**, *9*, 117.
(310) Seitz, M. Force spectroscopy. In *Nanobiotechnology*; Niemeyer, C. M., Mirkin, C., Eds.; Wiley-VCH: Weinheim, Germany, 2004.
(311) Albrecht, C.; Blank, K.; Lalic-Multhaler, M.; Hirler, S.; Mai, T.; Gilbert, I.; Schiffmann, S.; Bayer, T.; Clausen-Schaumann, H.; Gaub, H. E. *Science* **2003**, *301*, 367.
(312) Viani, M. B.; Schaffer, T. E.; Chand, A.; Rief, M.; Gaub, H. E.; Hansma, P. K. *J. Appl. Phys.* **1999**, *86*, 2258.
(313) Gittes, F.; Schmidt, C. F. *Eur. Biophys. J. Biophys. Lett.* **1998**, *27*, 75.
(314) Binnig, G.; Quate, C. F.; Gerber, C. *Phys. Rev. Lett.* **1986**, *56*, 930.
(315) Kishino, A.; Yanagida, T. *Nature* **1988**, *334*, 74.
(316) Lantz, M. A.; Hug, H. J.; Hoffmann, R.; van Schendel, P. J. A.; Kappenberger, P.; Martin, S.; Baratoff, A.; Güntherodt, H. J. *Science* **2001**, *291*, 2580.
(317) Jarvis, S. P.; Yamada, H.; Yamamoto, S. L.; Tokumoto, H.; Pethica, J. B. *Nature* **1996**, *384*, 247.
(318) Erlandsson, R.; Yakimov, V. *Phys. Rev. B* **2000**, *62*, 13680.
(319) Buldum, A.; Ciraci, S.; Fong, C. Y.; Nelson, J. S. *Phys. Rev. B* **1999**, *59*, 5120.
(320) Hänggi, P.; Talkner, P.; Borkovec, M. *Rev. Mod. Phys.* **1990**, *62*, 251.
(321) Evans, E.; Ritchie, K. *Biophys. J.* **1997**, *72*, 1541.
(322) Grandbois, M.; Beyer, M.; Rief, M.; Clausen-Schaumann, H.; Gaub, H. E. *Science* **1999**, *283*, 1727.
(323) Beyer, M. K. *J. Chem. Phys.* **2000**, *112*, 7307.
(324) Röhrig, U. F.; Frank, I. *J. Chem. Phys.* **2001**, *115*, 8670.
(325) Pérez, R.; Stich, I.; Payne, M. C.; Terakura, K. *Phys. Rev. B* **1998**, *58*, 10835.
(326) Pérez, R.; Payne, M. C.; Stich, I.; Terakura, K. *Phys. Rev. Lett.* **1997**, *78*, 678.
(327) Rubio, G.; Agrait, N.; Vieira, S. *Phys. Rev. Lett.* **1996**, *76*, 2302.

(328) Rubio-Bollinger, G.; Bahn, S. R.; Agrait, N.; Jacobsen, K. W.; Vieira, S. *Phys. Rev. Lett.* **2001**, *87*, 026101.
(329) Lantz, M. A.; Hug, H. J.; van Schendel, P. J. A.; Hoffmann, R.; Martin, S.; Baratoff, A.; Abdurixit, A.; Güntherodt, H. J.; Gerber, C. *Phys. Rev. Lett.* **2000**, *84*, 2642.
(330) Giessibl, F. J. *Appl. Phys. Lett.* **2001**, *78*, 123.
(331) Guggisberg, M.; Bammerlin, M.; Loppacher, C.; Pfeiffer, O.; Abdurixit, A.; Barwich, V.; Bennewitz, R.; Baratoff, A.; Meyer, E.; Güntherodt, H. J. *Phys. Rev. B* **2000**, *61*, 11151.
(332) Dürig, U. *Appl. Phys. Lett.* **2000**, *76*, 1203.
(333) Gotsmann, B.; Anczykowski, B.; Seidel, C.; Fuchs, H. *Appl. Surf. Sci.* **1999**, *140*, 314.
(334) Giessibl, F. J. *Phys. Rev. B* **1997**, *56*, 16010.
(335) Sader, J. E.; Jarvis, S. P. *Appl. Phys. Lett.* **2004**, *84*, 1801.
(336) Hoffmann, R.; Lantz, M. A.; Hug, H. J.; van Schendel, P. J. A.; Kappenberger, P.; Martin, S.; Baratoff, A.; Güntherodt, H. J. *Phys. Rev. B* **2003**, 67.
(337) Uchihashi, T.; Sugawara, Y.; Tsukamoto, T.; Ohta, M.; Morita, S.; Suzuki, M. *Phys. Rev. B* **1997**, *56*, 9834.
(338) Hoffmann, P. M.; Oral, A.; Grimble, R. A.; Ozer, H. O.; Jeffery, S.; Pethica, J. B. *Proc. R. Soc. London, Ser. A* **2001**, *457*, 1161.
(339) Özer, H. Ö.; Atabak, M.; Ellialtioglu, R. M.; Oral, A. *Appl. Surf. Sci.* **2002**, *188*, 301.
(340) Bensimon, D.; Simon, A. J.; Croquette, V.; Bensimon, A. *Phys. Rev. Lett.* **1995**, *74*, 4754.
(341) Clausen-Schaumann, H.; Rief, M.; Tolksdorf, C.; Gaub, H. E. *Biophys. J.* **2000**, 78.
(342) Marszalek, P. E.; Oberhauser, A. F.; Pang, Y. P.; Fernandez, J. M. *Nature* **1998**, *396*, 661.
(343) Li, H.; Rief, M.; Oesterhelt, F.; Gaub, H. E.; Zhang, X.; Shen, J. *Chem. Phys. Lett.* **1999**, *305*, 197.
(344) Heymann, B.; Grubmuller, H. *Chem. Phys. Lett.* **1999**, *305*, 202.
(345) Lu, Z. Y.; Nowak, W.; Lee, G. R.; Marszalek, P. E.; Yang, W. T. *J. Am. Chem. Soc.* **2004**, *126*, 9033.
(346) Evans, E.; Ritchie, K. *Biophys. J.* **1999**, *76*, 2439.
(347) Friedsam, C.; Wehle, A. K.; Kuhner, F.; Gaub, H. E. *J. Phys.: Condens. Matter* **2003**, *15*, S1709.
(348) Krüger, D.; Fuchs, H.; Rousseau, R.; Marx, D.; Parrinello, M. *J. Chem. Phys.* **2001**, *115*, 4776.
(349) Krüger, D.; Fuchs, H.; Rousseau, R.; Marx, D.; Parrinello, M. *Phys. Rev. Lett.* **2002**, *89*, 186402.
(350) Merkel, R.; Nassoy, P.; Leung, A.; Ritchie, K.; Evans, E. *Nature* **1999**, *397*, 50.
(351) Garnier, L.; Gauthier-Manuel, B.; van der Vegte, E. W.; Snijders, J.; Hadziioannou, G. *J. Chem. Phys.* **2000**, *113*, 2497.
(352) de Boer, J. H. *Trans. Faraday Soc.* **1936**, *32*, 10.
(353) Pascual, J. I.; Mendéz, J.; Gómez-Herrero, J.; Baró, A. M.; García, N.; Binh, V. T. *Phys. Rev. Lett.* **1993**, *71*, 1852.
(354) Krans, J. M.; Muller, C. J.; Yanson, I. K.; van Ruitenbeek, J. M. *Physica B* **1994**, *194*, 1033.
(355) Agraït, N.; Rodrigo, J. G.; Vieira, S. *Phys. Rev. B* **1993**, *47*, 12345.
(356) Agraït, N.; Rubio, G.; Vieira, S. *Phys. Rev. Lett.* **1995**, *74*, 3995.
(357) Agraït, N.; Rubio, G.; Vieira, S. *Langmuir* **1996**, *12*, 4505.
(358) Landman, U.; Luedtke, W. D.; Gao, J. P. *Langmuir* **1996**, *12*, 4514.
(359) Landman, U.; Luedtke, W. D.; Salisbury, B. E.; Whetten, R. L. *Phys. Rev. Lett.* **1996**, *77*, 1362.
(360) Stalder, A.; Durig, U. *Appl. Phys. Lett.* **1996**, *68*, 637.
(361) Stalder, A.; Durig, U. *J. Vac. Sci. Technol. B* **1996**, *14*, 1259.
(362) Landman, U.; Barnett, R. N.; Luedtke, W. D. *Z. Phys. D: At., Mol. Clusters* **1997**, *40*, 282.
(363) Ohnishi, H.; Kondo, Y.; Takayanagi, K. *Nature* **1998**, *395*, 780.
(364) Yanson, A. I.; Rubio Bollinger, G.; van den Brom, H. E.; Agraït, N.; van Ruitenbeek, J. M. *Nature* **1998**, *395*, 783.
(365) Sánchez-Portal, D.; Artacho, E.; Junquera, J.; Ordejón, P.; García, A.; Soler, J. M. *Phys. Rev. Lett.* **1999**, *83*, 3884.
(366) Marszalek, P. E.; Greenleaf, W. J.; Li, H. B.; Oberhauser, A. F.; Fernandez, J. M. *Proc. Natl. Acad. Sci. U.S.A.* **2000**, *97*, 6282.
(367) Novaes, F. D.; da Silva, A. J. R.; da Silva, E. Z.; Fazzio, A. *Phys. Rev. Lett.* **2003**, *90*, 036101.
(368) da Silva, E. Z.; Novaes, F. D.; da Silva, A. J. R.; Fazzio, A. *Phys. Rev. B* **2004**, *69*, 115411.
(369) Rubio-Bollinger, G.; Joyez, P.; Agraït, N. *Phys. Rev. Lett.* **2004**, *93*, 116803.
(370) Rose, J. H.; Smith, J. R.; Ferrante, J. *Phys. Rev. B* **1983**, *28*, 1835.
(371) Conti, M.; Falini, G.; Samori, B. *Angew. Chem. Int. Ed.* **2000**, *39*, 215.
(372) Schmitt, L.; Ludwig, M.; Gaub, H. E.; Tampe, R. *Biophys. J.* **2000**, *78*, 3275.
(373) Kienberger, F.; Kada, G.; Gruber, H. J.; Pastushenko, V. P.; Riener, C. K.; Trieb, M.; Knaus, H.-G.; Schindler, H.; Hinterdorfer, P. *Single Mol.* **2000**, *1*, 59.
(374) Kado, S.; Kimura, K. *J. Am. Chem. Soc.* **2003**, *125*, 4560.
(375) Zapotoczny, S.; Auletta, T.; de Jong, M. R.; Schonherr, H.; Huskens, J.; van Veggel, F.; Reinhoudt, D. N.; Vancso, G. J. *Langmuir* **2002**, *18*, 6988.
(376) Schonherr, H.; Beulen, M. W. J.; Bugler, J.; Huskens, J.; van Veggel, F.; Reinhoudt, D. N.; Vancso, G. J. *J. Am. Chem. Soc.* **2000**, *122*, 4963.
(377) Auletta, T.; de Jong, M. R.; Mulder, A.; van Veggel, F.; Huskens, J.; Reinhoudt, D. N.; Zou, S.; Zapotoczny, S.; Schonherr, H.; Vancso, G. J.; Kuipers, L. *J. Am. Chem. Soc.* **2004**, *126*, 1577.
(378) Essevaz-Roulet, B.; Bockelmann, U.; Heslot, F. *Proc. Natl. Acad. Sci. U.S.A.* **1997**, *94*, 11935.
(379) Rief, M.; Clausen-Schaumann, H.; Gaub, H. E. *Nat. Struct. Biol.* **1999**, *6*, 346.
(380) Lehn, J. M. *Angew. Chem., Int. Ed. Engl.* **1990**, *29*, 1304.
(381) Kudera, M.; Eschbaumer, C.; Gaub, H. E.; Schubert, U. S. *Adv. Funct. Mater.* **2003**, *13*, 615.
(382) Skulason, H.; Frisbie, C. D. *J. Am. Chem. Soc.* **2002**, *124*, 15125.
(383) Seifert, U. *Phys. Rev. Lett.* **2000**, *84*, 2750.
(384) Stasiak, A.; Dobay, A.; Dubochet, J.; Dietler, G.; Gaub, H. E.; Clausen-Schaumann, H.; Beyer, M.; Rief, M.; Grandbois, M. *Science* **1999**, *286*, 11a.
(385) Deguchi, T.; Tsurusaki, K. *Phys. Rev. E* **1997**, *55*, 6245.
(386) Arai, Y.; Yasuda, R.; Akashi, K.; Harada, Y.; Miyata, H.; Kinosita, K.; Itoh, H. *Nature* **1999**, *399*, 446.
(387) Tsuda, Y.; Yasutake, H.; Ishijima, A.; Yanagida, T. *Proc. Natl. Acad. Sci. U.S.A.* **1996**, *93*, 12937.
(388) Bao, X. Y. R.; Lee, H. J.; Quake, S. R. *Phys. Rev. Lett.* **2003**, *91*, 265506.
(389) Saitta, A. M.; Soper, P. D.; Wasserman, E.; Klein, M. L. *Nature* **1999**, *399*, 46.
(390) Saitta, A. M.; Klein, M. L. *J. Chem. Phys.* **1999**, *111*, 9434.
(391) Saitta, A. M.; Klein, M. L. *J. Am. Chem. Soc.* **1999**, *121*, 11827.
(392) Saitta, A. M.; Klein, M. L. *J. Phys. Chem. B* **2000**, *104*, 2197.
(393) Saitta, A. M.; Klein, M. L. *J. Phys. Chem. B* **2001**, *105*, 6495.
(394) Saitta, A. M.; Klein, M. L. *J. Chem. Phys.* **2002**, *116*, 5333.
(395) Kim, E. G.; Klein, M. L. *Macromolecules* **2004**, *37*, 1674.
(396) Farago, O.; Kantor, Y.; Kardar, M. *Europhys. Lett.* **2002**, *60*, 53.
(397) Dommersnes, P. G.; Kantor, Y.; Kardar, M. *Phys. Rev. E* **2002**, *66*, 031802.
(398) Badger, R. M. *J. Chem. Phys.* **1934**, *2*, 128.
(399) Aktah, D.; Frank, I. *J. Am. Chem. Soc.* **2002**, *124*, 3402.

CR030697H